

The Drag-Free Satellite

BENJAMIN LANGE*

Lockheed Missiles and Space Company, Palo Alto, Calif.

A scientific earth satellite that is guided in a drag-free orbit by a shielded, free-falling proof mass has been proposed by a number of investigators. This paper examines the feasibility and some of the applications of this scheme. The control and guidance system is analyzed with respect to system performance and gas usage requirements. The principal trajectory errors that are due to vehicle gravity, stray electric and magnetic fields, and sensor forces are investigated. It is found that drag and solar radiation pressure forces may be effectively reduced by three to five orders of magnitude for 100- to 500-mile orbits and that the deviation from a purely-gravitational orbit may be made as small as 1 m/yr. Such a satellite could be used to make precise measurements in geodesy and aeronomy; and, if a spherical proof mass is spun as a gyroscope, its random drift rate would probably be less than 0.1 sec-arc/yr. Such a gyroscope could be used to measure the effects that would ultimately limit the performance of the best terrestrial or satellite-borne gyros, and it might also be good enough to perform the experiment proposed by G. E. Pugh and L. I. Schiff to test general relativity.

Nomenclature

A	= direction cosine matrix	el, e_2	= gyrorotor eccentricities
A_B	= ball projected area	\mathbf{e}_ω	= unit vector parallel to ω_B
A_C	= area of capacitive plates	\mathbf{F}_{GS}	= control force on the satellite
A_S	= satellite projected area	\mathbf{F}_D	= all terms on the right side of Eq. (6) except $-(m_B/m_S)\mathbf{F}_{GS}$
A, B, C	= principal moments of inertia of gyrorotor	\mathbf{F}_{drag}	= aerodynamic drag force plus solar radiation force
a	= satellite orbit semimajor axis	\mathbf{F}_{GB}	= force of gravity on the ball
a, b, c	= ellipsoidal principal axes of gyrorotor	\mathbf{F}_{GS}	= \mathbf{F}_{Gk} = force of gravity on the satellite
B	= magnetic induction vector	$\Delta\mathbf{F}_G$	= $\mathbf{F}_{GB} - (m_B/m_S)\mathbf{F}_{GS}$
B_e	= earth's magnetic induction	\mathbf{F}_S	= any force acting on the satellite
\mathbf{B}_0	= uniform external field in the absence of the rotor	\mathbf{F}_{PB}	= any nongravitational force on the ball except those due to the satellite
B_0'	= component of \mathbf{B}_0 along a given rotor principal axis	\mathbf{F}_{PS}	= sum of all forces on the satellite except those due to gravity and drag
B_{11}	= component of B parallel to ω_B	\mathbf{F}_{SB}	= force that the satellite exerts on the ball
B_\perp	= component of B perpendicular to ω_B	f	= a specific force or acceleration, \mathbf{F}/m
b	= atmospheric rotation resistance coefficient	f_C	= control acceleration, $-(1/m_S)\mathbf{F}_C$
C_D	= drag coefficient	f_D	= disturbing acceleration, $-(1/m_S)\mathbf{F}_D$
c	= speed of light in vacuum	f_{DB}	= $f_{PB} + f_{SB}$
D_n	= normalized drag force	f_{DBas}	= specific force on the ball due to random molecular collisions
d, d_2	= a distance characteristic of vehicle size	$f_{DB\xi}, f_{DB\eta}, f_{DB\zeta}$	= components of f_{DB} along the ξ, η, ζ axes
d_b	= width of light beam	f_{GB}	= gravitational acceleration on the ball, \mathbf{F}_{GB}/m_B
d_1	= cavity radius or characteristic size	f_{SB}	= \mathbf{F}_{SB}/m_B
d_g	= capacitive pickup gap size	f_{PB}	= \mathbf{F}_{PB}/m_B
Δd_g	= departure of proof mass from the point where the electric forces from a capacitive pickup are zero	G	= universal gravitational constant
E	= eccentric anomaly or electric field or Young's modulus	g_H	= gyromagnetic ratio of a material
E_{av}	= average value of the electric field over the surface of the proof mass	g_e	= acceleration of gravity at the earth's surface
E_{max}	= maximum value of the electric field over the surface of the proof mass	H	= pressure scale height or magnetic field
E_n	= normal component of electric field	\mathbf{H}_0	= \mathbf{B}_0/μ_0
e	= eccentricity of the satellite orbit or of the gyrorotor considered as an oblate spheroid or electronic charge	H_0''	= component of \mathbf{H}_0 along a given rotor principal axis
e/m	= charge to mass ratio of the electron	H_R	= scale height at reference attitude h_R
		h	= altitude
		h_B	= angular momentum of the ball
		h_P	= perigee altitude
		h_R	= reference altitude at which the atmospheric density scale height is linearized
		h_S	= length of cylindrical satellite
		I_{sp}	= control gas specific impulse
		I_1, I_2, I_3	= satellite principal moments of inertia
		k	= reciprocal slope of contactor switching line or Boltzmann constant
		K, K_2	= cf. Eqs. (B1-B5)
		K_C	= cf. Eq. (B19)
		\mathbf{M}_P	= position feedback gain
		\mathbf{M}_V	= velocity feedback gain
			= moment or torque vector
		M_{Bx}, M_{By}, M_{Bz}	= components of the gyrorotor torques
		M_{11}	= component of M parallel to ω_B
		m_\perp	= component of M perpendicular to ω_B

Presented as Preprint 62-111 at the IAS Annual Summer Meeting, Los Angeles, Calif., June 19-22, 1962; revision received May 26, 1964. This work was based on research done at Stanford University, Stanford, Calif. and was supported by the Lockheed Missiles and Space Company. This research was associated with a program at Stanford supported by a NASA grant. The author wishes to acknowledge the help of Robert H. Cannon Jr. of Stanford University, who helped to clarify many of the concepts in this paper through numerous conversations.

*Graduate Study Engineer/Scientist; now Assistant Professor of Aeronautics and Astronautics, Stanford University, Stanford, Calif. Member AIAA.

m_{av} = average molecular mass of the atmosphere in the satellite

m_B = mass of the ball, proof mass, or gyrorotor

m_E = mass of earth

m_g = mass of control gas

$m_g(T)$ = mass of control gas expelled in time T

m_H = magnetic moment

m_{HB} = magnetic moment of the ball

m_{HS} = magnetic moment of the satellite

m_S = mass of the satellite and control gas

ρ = atmospheric velocity resistance coefficient

q_B = charge on the ball

R_B = radius of the ball or gyrorotor

R_e = radius of the earth

r = radius vector

$r_B, r_{BK}, r_C, r_{CB}, r_{CZ}, r_{EB}, r_{EK}, r_{IB}, r_{IS}, r_S, r_{SB}, r_{SC}, r_{ZB}$ = all defined by Fig. 1

r_{ES} = radius vector from earth to satellite

r_Q = distance to a point charge from the center of a spherical cavity

r_R = radius from earth's center to reference altitude $r_R = R_e + h_R$

r_C, r_C' = r_C written as column matrices in rotating and nonrotating reference frames, respectively

SB = surface area of the gyrorotor

T = period of one control limit cycle or absolute temperature

T_C = time when control is on

T_D = time when control is off

T_{FL} = fuel lifetime

T_L = time lag

T_O = orbit period

T_W = period of one limit cycle when $f_D = 0$

T_{CW} = total time control is on during T_W

T_r = translation control time constant

T_ω = attitude or rotation control time constant

T_1, T_2 = noise filter time constants

t = time

ti = assumed thickness or depth of penetration of surface eddy currents

t_{DB} = time after perigee passage when the control limit cycle first begins to saturate

V_B = potential between the ball and the cavity

V_C = capacitive pickup input voltage

v_O = velocity of the satellite in orbit

W = light power incident on the ball

W_g = weight of the control gas

W_{gw} = weight of the wasted control gas

x_L, x_R, x_S, x_B, x_T = limit cycle points defined by Fig. 5

x_B, y_B, z_B = gyrorotor principal axes

x_C, y_C, z_C = components of r_C

α = slope of the density scale height curve

β = $(1 + \alpha)/\alpha$

α, β, γ = angles between w_B and x_B, y_B, z_B

δ = contactor threshold level

$\epsilon, \epsilon_1, \epsilon_2$ = gyrorotor ellipticities

ϵ_0 = permittivity of free space

ϵ_P = ellipticity due to a built in or permanent bulge

ϵ_R = ellipticity due to a bulge caused by rotation

θ_{max} = equivalent initial attitude rate caused by an impulsive disturbance

μ_0 = permeability of free space

ξ, η, ζ = rotating locally level system of relative coordinates with their origin in a nominal circular orbit about the earth

P = atmospheric mass density

ρ_R = atmospheric mass density at the reference altitude

ρ_m = mass density of the proof mass or gyrorotor

σ = gyrorotor electrical conductivity

σ_x = rms position error

σ_z = rms velocity error

ϕ = angle of the gyrospin axis with respect to some initial reference or gravitational potential function

ϕ_2 = second term in series expansion of gravitational potential of the satellite

$\dot{\phi}_{peak}$ = peak precession rate of the gyrospin axis

$\langle \phi^2 \rangle_{av}$ = mean square value of ϕ when the gyro is disturbed by random atmospheric torques

χ_m = magnetic susceptibility of isotropic material

χ_m = magnetic susceptibility tensor of anisotropic material

χ_m', χ_m'' = two of the eigenvalues of χ_m for the primed and double primed axes, respectively

ψ = angle between ω_B and h_B

ω_B = angular velocity of the gyrorotor

$\omega_{Bz}, \omega_{By}, \omega_{Bx}$ = components of ω_B in the rotor principal axes

ω_O = orbit angular velocity

ω_S = satellite angular velocity

$\omega_x, \omega_y, \omega_z$ = components of ω_S in the satellite principal axes

Subscripts

B = ball (proof mass or gyrorotor) or bottom

b = beam

C = control center, control, capacitive

D = disturbing

DB = deadband

drag = atmospheric drag plus solar radiation force

E, e = earth

FL = fuel lifetime

G = gravitational

g = gas or gap

H = magnetic

I = inertial

K = center of gravity

L = left or lag

m = mass

n = normal

O = orbit

P = perturbing or permanent or position or perigee

Q = charge

R = right or reference or rotation

r = translation

S = satellite or switch

T = top

V, x = vehicle or velocity

x = position

Z = zero self-gravity

ω = rotation

Introduction

THE term "drag-free satellite" as used in this paper will refer to a small spherical proof mass or ball inside of a completely enclosed cavity in a larger satellite. The outer satellite has a jet activated translation control system that causes it to pursue the proof mass such that the two never touch. Since the cavity is closed, the ball is shielded from gas drag and solar radiation pressure; and, in the ideal case when the effects of other disturbing forces are negligible, the orbit of the proof mass will be determined only by the forces of gravity. The only disturbing forces that can act on the proof mass will arise from the satellite itself or from any interactions that can penetrate the shield. Forces due to the satellite can arise from vehicle gravity, stray electric and magnetic fields, and the interaction of the position sensor.

A similar technique was first used by researchers into the state of weightlessness.¹ Airplanes were flown in weightless trajectories by keeping a small object centered in free space in the cabin. The same system has also been suggested as a guidance scheme to cause ballistic missiles to re-enter along a path that is undisturbed by aerodynamic forces. Erikké² also has suggested launching a half-airplane half-satellite that would fly at altitudes between 90 and 180 km and use some thrust to cancel drag. He calls such a vehicle a "sateloid" and points out that it may also fly at subcircular velocities using aerodynamic lift to sustain it.

The first suggestions of this scheme purely in connection with a satellite apparently were made independently from

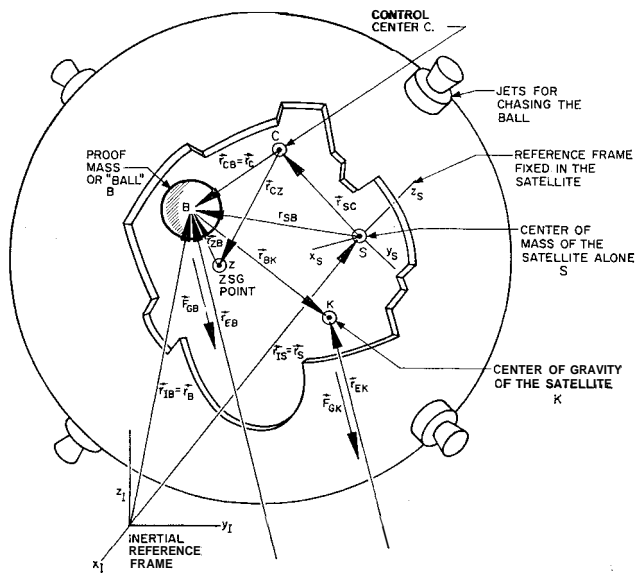


Fig. 1 Drag-free satellite geometry.

1959 to 1961 by a number of investigators. Schwarzschild³ at Princeton, Ferrell (in an unpublished report),¹⁰ Pugh⁴ and MacDonald⁵ at The University of California at Los Angeles have proposed various forms of the drag-free satellite. It was also suggested independently by C. W. Sherwin of Aerospace and by the author at the Stanford Conference on Experimental Tests of Theories of Relativity in July 1961.⁶ Several possible uses or missions for such a satellite have been proposed.

1. *Geodesy*: The departure of the figure of the earth from a perfect sphere introduces higher harmonics in the earth's gravitational potential. These harmonics perturb earth satellite orbit elements, and it is possible to measure the harmonics of the earth's gravitational field by observing the changes in a satellite's orbit elements. However, the atmosphere also perturbs the satellite elements, and this effect must be corrected out in accurate geodetic measurements. These techniques are explained in detail by Kaula.⁷ A drag-free satellite would remove the necessity of correcting for the uncertainties of atmospheric drag and solar radiation pressure in satellite observations of the higher harmonics of the earth's gravitational field. In addition, operation would be possible at lower altitudes where the effects of higher harmonics are stronger, but this advantage must be weighed against shorter fuel lifetime.

2. *Aeronomy*: Conventional upper atmosphere density measurements* depend on observing the change in the satellite period over several orbits and essentially determine the average density over this time and altitude range. This type of data is not as useful as instantaneous density measurements. The proof mass in the satellite essentially constitutes a very sensitive accelerometer that could be used to measure the instantaneous gas drag and radiation pressure at any altitude. For a spherically shaped satellite, $C_D \rightarrow 2$ in free molecular flow at high Mach numbers regardless of the accommodation coefficient; and the calibration of the instrument would not depend on knowing the accommodation coefficient as does, for example, Sharp's density gage.⁹ The actual drag forces may be inferred from the jet plenum chamber temperatures and pressures, from the relative motion between the proof mass and the satellite, or may be measured by measuring the forces between the jets and the satellite with strain gages. The latter technique is feasible because the jet forces are typically one to three orders of magnitude larger than the drag force because the jets are on for only a small fraction of the total time.

3. *Precision gyroscopes*: If the spherical proof mass is spun at a very rapid rate, it becomes a gyroscope. Since

there are no support forces, the only disturbing torques arise from gravity gradient effects, electromagnetic interactions, relativity effects, and readout torques. It appears possible to construct a gyroscope whose random drift rates would be less than 0.1 sec-arc/yr. Such an instrument would be very useful to study the effects not connected with the support forces which would ultimately become important in the construction of extremely low-drift gyroscopes, and it would be possible to do this many years in advance of the time when it might be possible to construct such instruments on earth.

4. *The Pugh-Schiff gyroscope experiment*: Schiff¹⁰ has shown that, although Newtonian theory predicts no precession of the spin axis of a spherically symmetric gyroscope in free-fall about the earth, general relativity predicts a geodetic precession arising from motion through the earth's gravitational field and a Lense-Thirring precession due to the difference between the gravitational field of a rotating and non-rotating earth. The geodetic precession in a satellite is about 7 sec-arc/yr, and the Lense-Thirring precession is about 0.1 sec-arc/yr. The design and preliminary development of this experiment in a satellite has been under way at Stanford University for about two years, and it is described by Cannon.¹¹

5. *Time dependence of gravity*: Dicke³ has suggested that such a satellite could be used as a clock whose rate would depend on the universal constant of gravity G . Such a clock could be compared to precision atomic clocks on earth. Any change in the rate of the gravitational clock could be interpreted as a change in the "constant" G . The value of G as a function of time has important consequences in the theories of relativity. The tracking accuracies necessary for this experiment are dictated by the very small size of the effect (about one part in 10^{10} /yr), which yields an accumulated lag in the satellite's position of about 0.2 sec-arc/yr. This is discussed in Ref. 12 in detail.

6. *Orbit sustaining*: For certain missions, it is desirable to operate at very low altitudes. Such a satellite would quickly re-enter if its drag were not counteracted in some manner. Rider,¹³ Bruce,¹⁴ and Roberson¹⁵ have discussed various ways of doing this. The freefalling ball could be used to control thrust such that the satellite would remain in orbit longer than it would without drag cancellation. This technique also would be especially useful to control precisely the entry points of satellites and large potentially dangerous spent booster stages. It also could be used to establish a true equiperiod orbit (where the orbit dips very low into the atmosphere) for rendezvous practice.

7. *Zero-g laboratories*: It has been proposed that the central parts of manned space stations be used as zero-g laboratories. For experiments of long duration, such a drag cancellation scheme would be necessary to prevent the apparatus from contacting the laboratory walls. This paper will examine some of the problems associated with the design and use of drag-free satellites.

Equations of Motion

The object of this section is to derive the relevant equations of motion that will be used in the analysis and synthesis of the control systems and in the computation of the magnitude and effects of the system errors.

General Equations

Figure 1 shows the geometry for a satellite with a proof mass in freefall and with three-axis translation control. In general, the center of mass and the center of gravity of the satellite do not coincide; and, in addition, the center of gravity is not even fixed in the body but is a function of body orientation. Furthermore, although the design objective would be to make the control center (the point at which the

position indicator reads zero, or, equivalently, the point to which the control system tries to drive the ball), the center of mass, and a point of zero self-gravity? all coincide; because of various uncertainties, these points will not be the same and the variations cannot be neglected.

If the vectors \mathbf{r}_{IB} , \mathbf{r}_{IS} , and \mathbf{r}_{CB} are abbreviated as \mathbf{r}_B , \mathbf{r}_S , and \mathbf{r}_C , respectively, the equation of motion of the proof mass or ball is

$$m_B \ddot{\mathbf{r}}_B = \mathbf{F}_{GB} + \mathbf{F}_{SB} + \mathbf{F}_{PB} \quad (1)$$

and the equation of motion of the center of mass of the satellite is

$$m_S \ddot{\mathbf{r}}_S = \mathbf{F}_{GS} + \mathbf{F}_{PS} + \mathbf{F}_{CS} - \mathbf{F}_{SB} \quad (2)$$

Since $\mathbf{r}_B = \mathbf{r}_S + \mathbf{r}_{SB}$, (1) and (2) may be combined to yield the equation of the ball in relative vehicle coordinates

$$m_B \ddot{\mathbf{r}}_{SB} = \left(\mathbf{F}_{GB} - \frac{m_B}{m_S} \mathbf{F}_{GS} \right) + \left(1 + \frac{m_B}{m_S} \right) \mathbf{F}_{SB} + \left(\mathbf{F}_{PB} - \frac{m_B}{m_S} \mathbf{F}_{PS} \right) - \frac{m_B}{m_S} \mathbf{F}_{CS} \quad (3)$$

Notice that, when the equation is written in this form, any forces applied to the satellite appear to be applied to the proof mass through the scale factor $(-m_B/m_S)$. It will often be convenient to speak of "applying a force to the proof mass," and this terminology will mean $-(m_B/m_S)\mathbf{F}_S$ whenever the force is actually applied to the satellite.

Whereas the vector \mathbf{r}_{SB} describes the position of the proof mass with respect to the center of mass of the satellite, the position sensing apparatus in the satellite actually measures the vector \mathbf{r}_C where $\mathbf{r}_{SB} = \mathbf{r}_{SC} + \mathbf{r}_C$. The vector \mathbf{r}_{SC} will be assumed to be fixed in the satellite; or equivalently, it will be assumed that the relative motion of the center of mass and the control center during the expulsion of gas may be neglected.

With this assumption, the equations of motion now become

$$m_B(\ddot{\mathbf{r}}_{SC} + \ddot{\mathbf{r}}_C) = \Delta \mathbf{F}_G + \left(1 + \frac{m_B}{m_S} \right) \mathbf{F}_{SB} + \left(\mathbf{F}_{PB} - \frac{m_B}{m_S} \mathbf{F}_{PS} \right) - \frac{m_B}{m_S} \mathbf{F}_{CS} \quad (4)$$

where

$$\Delta \mathbf{F}_G \triangleq [\mathbf{F}_{GB} - (m_B/m_S)\mathbf{F}_{GS}]$$

Because of the rotation $\boldsymbol{\omega}_S$ of the satellite,

$$\ddot{\mathbf{r}}_{SC} + \ddot{\mathbf{r}}_C = \ddot{\mathbf{r}}_C + 2\boldsymbol{\omega}_S \times \dot{\mathbf{r}}_C + \dot{\boldsymbol{\omega}}_S \times (\mathbf{r}_C + \mathbf{r}_{SC}) + \boldsymbol{\omega}_S \times [\boldsymbol{\omega}_S \times (\mathbf{r}_C + \mathbf{r}_{SC})] \quad (5)\ddagger$$

and the relative translation equations, written in terms of the vector \mathbf{r}_C , measured by the position sensor, are

$$m_B[\ddot{\mathbf{r}}_C + 2\boldsymbol{\omega}_S \times \dot{\mathbf{r}}_C + \dot{\boldsymbol{\omega}}_S \times \mathbf{r}_C + \boldsymbol{\omega}_S \times (\boldsymbol{\omega}_S \times \mathbf{r}_C)] = m_B[-\dot{\boldsymbol{\omega}}_S \times \mathbf{r}_{SC} - \boldsymbol{\omega}_S \times (\boldsymbol{\omega}_S \times \mathbf{r}_{SC})] + \Delta \mathbf{F}_G + \left(1 + \frac{m_B}{m_S} \right) \mathbf{F}_{SB} + \left(\mathbf{F}_{PB} - \frac{m_B}{m_S} \mathbf{F}_{PS} \right) - \frac{m_B}{m_S} \mathbf{F}_{CS} \quad (6)$$

The special cases of Eq. (6) for various types of attitude control are given in Appendix A.

† A point of zero self-gravity or ZSG point is a point where all of the gravitational forces due to the satellite alone sum to zero (cf. Appendix B).

‡ For any vector such as \mathbf{r}_C , the notation $\dot{\mathbf{r}}_C$ will mean the time rate of change of \mathbf{r}_C seen by an observer in a reference frame that is nonrotating with respect to inertial space. The notation $\ddot{\mathbf{r}}_C$ will mean the time rate of change of \mathbf{r}_C seen by an observer in a reference frame that is nonrotating with respect to the satellite so that $\ddot{\mathbf{r}}_C = \ddot{\mathbf{r}}_C + \boldsymbol{\omega}_S \times \dot{\mathbf{r}}_C$.

The Forcing Terms and Their Relative Magnitudes

Since the satellite is constrained by the translation control system to follow the proof mass, the orbit of the satellite will be determined solely by Eq. (1). The proof mass will be disturbed from a purely gravitational orbit only by the terms \mathbf{F}_{SB} and \mathbf{F}_{PB} . These are shown in the section on trajectory error to correspond to accelerations that are less than $10^{-11}g_e$.§

The terms on the right-hand side of Eq. (6) determine the relative motion between the satellite and the ball, and their magnitudes are important only in the translation control system.

If one considers only the gravitational attraction of a spherical earth,

$$\Delta \mathbf{F}_G \triangleq \mathbf{F}_{GB} - \frac{m_B}{m_S} \mathbf{F}_{GS} \approx Gm_B m_B \left[\frac{\mathbf{r}_{BK}}{r_{EB}^3} - 3 \frac{\mathbf{r}_{EB}(\mathbf{r}_{EB} \cdot \mathbf{r}_{BK})}{r_{EB}^5} \right] \quad (7)$$

$$\Delta F_G \approx Gm_B m_B r_{BK} / r_{EB}^3 \quad (8)$$

$$\Delta f_G / g_e \triangleq \Delta F_G / m_B g_e \approx r_{BK} / r_{EB} \approx 10^{-10} \text{ to } 10^{-11} \quad (9)$$

Likewise it will be shown that, since $m_B/m_S \ll 1$,

$$(1/m_B)[1 + (m_B/m_S)]F_{SB} \approx 10^{-11}g_e \quad (10)$$

Finally,

$$\frac{1}{m_B} \left| \mathbf{F}_{PB} - \frac{m_B}{m_S} \mathbf{F}_{PS} \right| \approx \frac{-F_{\text{drag}}}{m_S} \approx 10^{-4} \text{ to } 10^{-8}g_e \quad (11)$$

Thus, for low orbits, the aerodynamic drag force \mathbf{F}_{drag} is the dominant translation disturbance, and, in order that the control keep the ball centered, the average control force must equal the average drag force:

$$\langle \mathbf{F}_{CS} \rangle_{\text{av}} \approx -\langle \mathbf{F}_{\text{drag}} \rangle_{\text{av}} \quad (12)$$

so that \mathbf{F}_{drag} may be measured by observing \mathbf{F}_{CS} .

Control Problem

The object of this section is to discuss the basic translation control problem (including fuel consumption) associated with the operation of a nonrotating drag-free satellite. The case where the satellite does not rotate with respect to an inertial reference is of interest for precision gyroscope experiments where the gyroscope spin axis must be compared with a fixed direction in inertial space. In addition, omitting the spin makes it easier to present the basic properties of the translation control without the added complexity due to the rotation. The control must accomplish two things: 1) keep the vector \mathbf{r}_C within some specified bound in the presence of the disturbing forces, and 2) do this with a minimum expenditure of fuel. The bound on \mathbf{r}_C will be dictated by the type of mission. For example, in the case of an aeronomy mission, it is merely necessary that the proof mass not contact the cavity walls very much, and, for geodesy experiments, the proof mass must be controlled in such a manner that the interactions between it and the satellite are as small as possible. For the precision gyroscope experiment, however, it is necessary that the rotor never contact the cavity walls; and, for some readout schemes, it is necessary that the rotor be very stationary with respect to the satellite during the readout period.

§ It is not correct to conclude immediately from these numbers that the drag is only cancelled to $10^{-11}g_e$ since the effect of \mathbf{F}_{SB} and \mathbf{F}_{PB} on the ball's orbit is not the same as the drag. This is true because the drag always acts along the velocity vector. See the section on "System Errors."

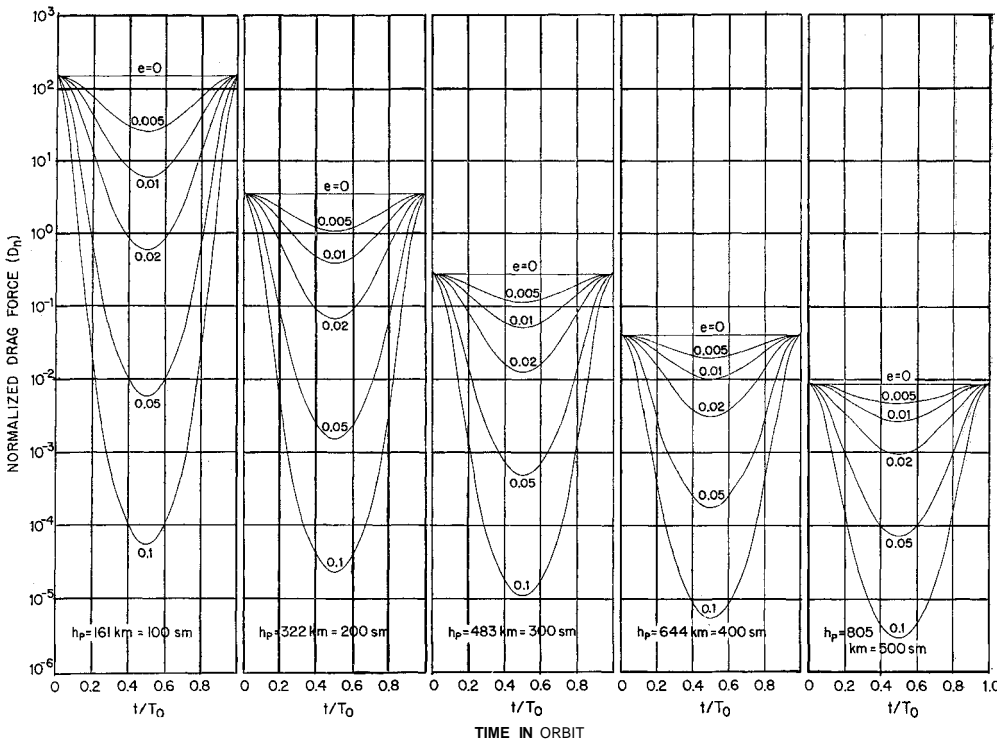


Fig. 2 Normalized drag computed from a linear scale height model of the atmosphere.

Disturbing Acceleration Due to Drag

If part of the subscripts are dropped, Eq. (A2) becomes

$$\ddot{x}_c = f_D + f_c \quad (13)$$

For most orbits, the dominant contribution to f_D is the atmospheric drag, and it is instructive to compute the drag as a function of time and orbit. The linear scale height model of the atmosphere as discussed by Smelt¹⁶ provides a more accurate representation than the conventional constant scale height exponential model and will be used in this calculation.

The drag force is given by

$$F_{\text{drag}} = 1/2 \rho v_0^2 C_D A_S \quad (14)$$

where the density ρ is obtained by integrating the hydrostatic equation using a scale height H , which varies linearly with altitude with slope α as shown in Eq. (15):

$$H = H_R + \alpha(h - h_R) \quad \beta \triangleq (1 + \alpha)/\alpha \quad (15)$$

$$\rho = \rho_R (H_R/H)^\beta (r_{ES}/r_R)^2 \quad (16)$$

$$r_{ES} = \alpha(1 - e \cos E) \quad (17)$$

$$v_0^2 = \omega_0^2 a^2 \frac{1 + e \cos E}{1 - e \cos E} = \frac{g_e R_e^2}{a} \frac{1 + e \cos E}{1 - e \cos E} \quad (18)$$

h_R is the reference altitude about which the scale height is linearized. Substituting (15-18) into (14) yields the normalized drag force D_n :

$$D_n \triangleq \frac{F_{\text{drag}}}{r_R A_S \rho_R g_e (C_D/2)} = \left(\frac{a}{r_R} \right) \left(\frac{R_e}{r_R} \right)^2 \times \frac{1 - e^2 \cos^2 E}{\{1 + [\alpha(a - r_R - ae \cos E)]/H_R\}^\beta} \quad (19)$$

Equation (19) is plotted in Fig. 2 using constants interpolated from the 1962 ARDC Model Atmosphere.¹⁷ The following values for the constants were assumed:

$$\left. \begin{aligned} h_R &= 400 \text{ km} = 250 \text{ statute miles} \\ H_R &= 76 \text{ km} = 47 \text{ statute miles} \\ R_e &= 6380 \text{ km} = 3960 \text{ statute miles} \\ \alpha &= \frac{1}{7} \\ \rho_R &= 65 \times 10^{-15} \text{ g/cm}^3 \end{aligned} \right\} \quad (20)$$

As an example, consider a satellite with $C_D = 2$ and $A_S = 0.5 \text{ m}^2 = 5.38 \text{ ft}^2$; then

$$r_R A_S \rho_R g_e = 2.15 \times 10^{-4} \text{ newtons} = 4.83 \times 10^{-5} \text{ lb} \quad (21)$$

and, if $m_S g_e = 445 \text{ newtons} = 100 \text{ lb}$, then $r_R A_S \rho_R g_e$ expressed in g_e 's is

$$r_R A_S \rho_R / m_S = 4.83 \times 10^{-7} \quad (22)$$

Thus $(R_e/r_R)^2$ times Eq. (22) gives the drag acceleration in a nominal circular orbit at the reference altitude of 400 km, and Eq. (21) or (22) may be used in conjunction with Fig. 2 to determine the drag forces for other orbits.

From the preceding considerations, it is clear that the control system will have to zero the proof mass in the presence of a disturbing force, which could vary several orders of magnitude over one orbit period depending on the eccentricity and perigee altitude.

Contactors Translation Control

Since leak-free valves for the control jets are most easily built when they are of the full-on or full-off type, it is convenient to use on-off or contactor translation control in the satellite. The general problem of using contactor control with linear switching to zero a dynamical plant is discussed in a number of basic control theory texts. See, for example, Flügge-Lotz¹⁸ or Graham and McRuer.¹⁹ The general state-of-the-art of contactor control is reviewed by Flügge-Lotz in Ref. 20.

The control of the nonrotating drag-free satellite is the same as the classical control problem discussed in the fore-mentioned references if the drag force is considered as a constant over one control limit cycle. For most orbits this is a reasonable assumption. The period of one limit cycle is approximately $\{[8(x_S + x_L)]/f_D\}^{1/2} = 40 \text{ sec}$ for $x_S + x_L = 0.1 \text{ cm}$ and $f_D = 5 \times 10^{-4} \text{ cm/sec}^2$.

As can be seen from Fig. 2, this number can vary from one to several thousand seconds. For simplicity it will be assumed in the following sections that f_D is approximately constant during this time interval although this is not true when $\{[8(x_S + x_L)]/f_D\}^{1/2}$ is of the same order as one orbit period.

Minimum Fuel Consumption Limit Cycles

When "on-off" or contactor control is used, there is nearly always the possibility of limit cycles near the origin due to threshold, dead-zone, and delay in the sensors and actuators. The effect of these limit cycles on gas consumption is an important question. Because of the presence of f_D , it is possible to find limit cycles that consume no more fuel than that which is required to offset the effect of f_D . Indeed, within certain limits, the amount of gas consumed is independent of the functional form of f_D . Since, for a gas jet,

$$F_C = -g_e I_{sp} \dot{m}_g \tag{23}$$

Eq. (13) becomes

$$m_B \ddot{x}_C = -(m_B/m_S) F_D + (m_B/m_S) g_e I_{sp} \dot{m}_g \tag{24a}$$

or

$$\dot{m}_g = (1/g_e I_{sp}) [F_D + m_S \ddot{x}_C] \tag{24b}$$

As long as the control always acts such that the sign of \dot{m}_g is the same as the sign of F_D (i.e., if the control always opposes the drag force), then, during any period of time when the sign of F_D does not change, $|\dot{m}_g|$ is either always $+ \dot{m}_g$ or always $- \dot{m}_g$. For definiteness assume that $F_D \geq 0$. Then $\dot{m}_g \geq 0$, and $|m| = m$ so that the total amount of fuel consumed in time T , $m_g(T)$ is given by

$$m_g(T) \triangleq \int_0^T |\dot{m}_g| dt = \int_0^T \dot{m}_g dt = \frac{1}{g_e I_{sp}} \left\{ \int_0^T F_D dt + m_S [\dot{x}_C(T) - \dot{x}_C(0)] \right\} \tag{25}$$

Under these circumstances, the value of $m_g(T)$ depends only on the right side of Eq. (25) and not on the functional form of \dot{m}_g . For the case of a limit cycle of period T , the gas consumed, $m_g(T)$, depends only on the integral

$$\int_0^T F_D dt$$

Furthermore,

$$\frac{1}{g_e I_{sp}} \int_0^T F_D dt$$

is the minimum amount of fuel needed during one period to hold the system in a limit cycle near the origin, and the system must consume this much fuel to balance out the effect of the drag force.

It is instructive to examine this in detail for the case where F_D is a constant. Figure 3 shows the phase plane plot of one possible limit cycle of period T bounded by a maximum excursion ($x_R - x_L$). The control jet switches on when $x_C = x_S$ and $\dot{x}_C = \dot{x}_T$ and switches off at $x_C = x_B$ and $\dot{x}_C = \dot{x}_B$.

The gas used per cycle is

$$m_g(T) = \frac{-F_C T_C}{g_e I_{sp}} = \frac{-F_C T}{g_e I_{sp}} \cdot \frac{T_C}{T_C + T_D} = \frac{-F_C T}{g_e I_{sp}} \cdot \frac{1}{1 + (T_D/T_C)} \tag{26}$$

However, since the time is given by $(\dot{x}_T - \dot{x}_B)$ divided by the acceleration

$$-T_C(F_C + F_D) = T_D F_D$$

so that

$$T_D/T_C = -(F_C + F_D)/F_D \tag{27}$$

and, by substituting (27) into (26), the gas consumed per limit cycle is

$$m_g(T) = F_D T / g_e I_{sp} \tag{28}$$

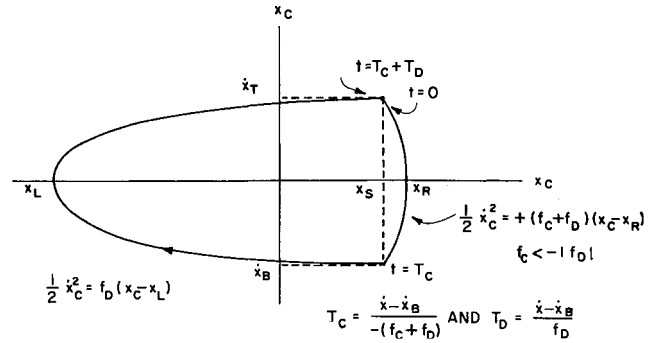


Fig. 3 Typical control limit cycle.

As long as the control force always opposes F_D , the gas consumed does not depend on the shape of the control force impulse but only on its area, which must be equal to $F_D T$. This very simple but important result makes it possible to compute the total fuel consumption by integrating the drag force over a complete orbit:

$$\begin{aligned} \frac{m_g}{\text{orbit}} &= \frac{1}{g_e I_{sp}} \int_0^{T_0} F_{\text{drag}} dt = \\ &= \frac{T_0}{2\pi g_e I_{sp}} \int_0^{2\pi} F_{\text{drag}} (1 - e \cos E) dE = \\ &= r_R A_S \rho_R \left(\frac{T_0}{I_{sp}} \right) \left(\frac{C_D}{2} \right) \left(\frac{a R_e^2}{r_R^3} \right) \frac{1}{2\pi} \times \\ &= \int_0^{2\pi} \frac{(1 - e \cos E - e^2 \cos^2 E + e^3 \cos^3 E) dE}{\{1 + [\alpha(a - r_R - ae \cos E)]/H_R\}^2} \tag{29} \end{aligned}$$

Surprisingly, this integral is fairly easy to evaluate by contour integration. Figure 4 shows a series of fuel lifetime plots obtained by evaluating this integral.

Bruce¹⁴ has computed the fuel expenditure necessary to sustain a satellite in a drag-free circular orbit. He compares continuous correction with a series of discrete corrections in which the orbit is allowed to decay for a fixed period of time and then is restored with a Hohman transfer. He concludes that continuous correction requires less fuel than the series of discrete corrections. This result also follows from the conclusion of the previous section since the control force acts in the same direction as the drag force during the second corrective impulse of a Hohman transfer and since the discrete application allows the orbit to decay into the denser atmosphere.

Control with Linear Switching, Threshold, and Deadband

In the previous sections it was shown that any control that does not allow the proof mass to touch the cavity walls and that always acts such as to oppose the drag will use the minimum amount of fuel, and this minimum was computed using a linear density scale height model of the atmosphere. The question arises how a control that has or approximates these properties might be mechanized. This section will consider one possible realization using linear switching, threshold, and deadband. ¶

Figure 5 shows typical switching surfaces in the phase plane with f_D always acting to the right. The finite width of the switching lines is due to contactor threshold that is built into the system as a design parameter δ . The loop time delay T_L , which is primarily due to the time required to operate the gas valves, is of the order of 5 to 25 msec and is negligible for most limit cycles. When the time delay is not negligible, its effect is to alter the vertical width of the switching line an amount $f_C T_L$ and to alter its slope by T_L/k^2 .

¶ For other approaches see Gaylord and Keller²¹ and Dahl, Aldrich, and Herman.²²

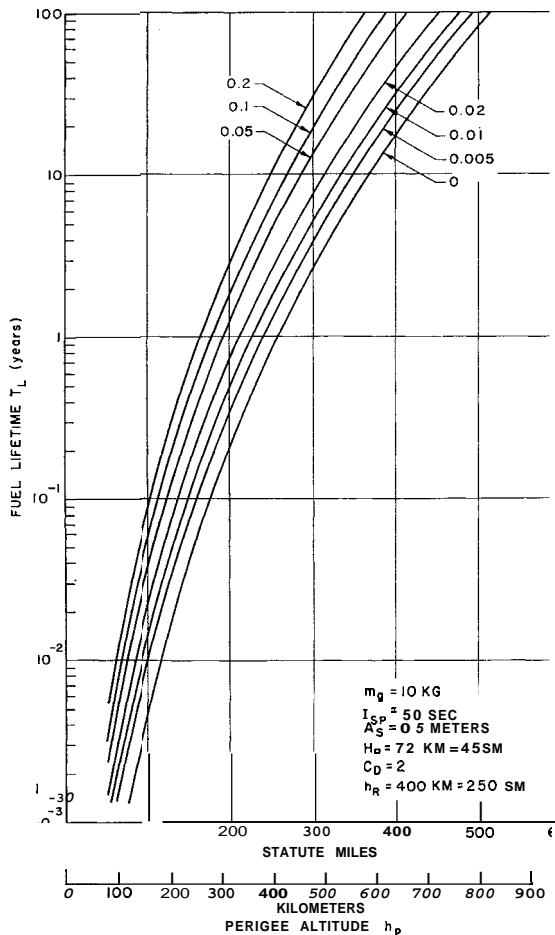


Fig. 4 Fuel lifetime of a drag-free satellite.

Thus, time delay limits the system only in that it establishes a minimum width of the switching line.

Table 1 shows several typical limit cycles for three perigee altitudes. It is assumed in all calculations that f_D is constant over one limit cycle. The minimum value of $x_S - x_L$ occurs at perigee and is chosen as 0.01 cm in this example. The first value for the drag acceleration in each block is the value obtained at perigee from Eq. (22) and Fig. 2, and it determines the required control acceleration and the size of $\dot{x}_T - \dot{x}_B$ and, hence, the value of δ since $\delta = 1/2k(\dot{x}_T - \dot{x}_B)$. Limit cycles for values of f_D equal to one-tenth and one-hundredth of that at perigee are also shown, and these correspond to higher altitudes in the orbit. A value of f_D which is 10^{-2} of that at perigee would, of course, bang

Table 1 Typical limit cycles for $1/s^2$ plant with drag (cf. Figs. 5 and 6)

h_p	f_D^a g_e 's	$x_S - x_L$ cm	$\dot{x}_T - \dot{x}_B^b$ cm/sec	T_D sec	$ f_C + f_D ^a$ g_e 's	$x_R - x_S$ cm	T_C msec	$\frac{T_C}{T_D}$
161 km or 100 statute miles	0.73×10^{-4}	10^{-2}	0.76×10^{-1}	1.1	0.93×10^{-3}	0.78×10^{-3}	82	7.8×10^{-2}
	0.73×10^{-5}	10^{-1}	0.76×10^{-1}	11	0.99×10^{-3}	0.74×10^{-3}	77	7.3×10^{-3}
	0.73×10^{-6}	1	0.76×10^{-1}	110	1.00×10^{-3}	0.73×10^{-3}	76	7.2×10^{-4}
	0	10^{-1}	0.76×10^{-1}	5.3	1.00×10^{-3}	0.73×10^{-3}	150 ^c	2.8×10^{-3}
322 km or 200 statute miles	1.7×10^{-6}	10^{-2}	1.2×10^{-2}	7	0.83×10^{-5}	2.2×10^{-3}	1500	2.2×10^{-1}
	1.7×10^{-7}	10^{-1}	1.2×10^{-2}	70	0.98×10^{-5}	1.9×10^{-3}	1200	1.7×10^{-2}
	1.7×10^{-8}	1	1.2×10^{-2}	700	1.0×10^{-5}	1.8×10^{-3}	1200	1.7×10^{-3}
	0	10^{-1}	1.2×10^{-2}	34	1.0×10^{-5}	1.8×10^{-3}	2300 ^c	7.8×10^{-2}
483 km or 300 statute miles	1.4×10^{-7}	10^{-2}	3.3×10^{-3}	24	1.0×10^{-5}	1.3×10^{-4}	330	1.4×10^{-2}
	1.4×10^{-8}	10^{-1}	3.3×10^{-3}	240	1.0×10^{-5}	1.3×10^{-4}	330	1.4×10^{-3}
	1.4×10^{-9}	1	3.3×10^{-3}	2400	1.0×10^{-5}	1.3×10^{-4}	330	1.4×10^{-4}
	0	10^{-1}	3.3×10^{-3}	120	1.0×10^{-5}	1.3×10^{-4}	660 ^c	5.5×10^{-3}

^a For a given orbit the drag at perigee determines the maximum value of f_D and hence the required value of f_C . Limit cycles are also shown for smaller values of f_D , which occur later in the orbit without giving the times or altitudes at which they occur.
^b $\dot{x}_T - \dot{x}_B$ is chosen to make $x_S - x_L = 10^{-2}$ cm at perigee and is constant over any given orbit.
^c When f_D is zero, the control acts at both ends of the limit cycle and hence T_C is longer.

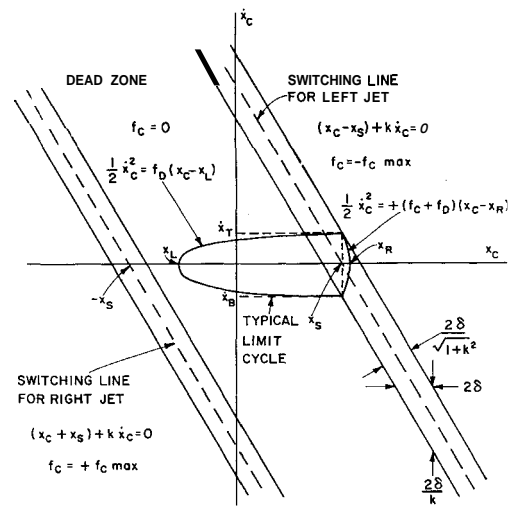


Fig. 5 On-off control switching lines.

against the left switching line, but the values corresponding to the full unsaturated limit cycle are shown here for comparison.

The last line in each block shows the values for saturated limit cycles where f_D is taken as zero. This limit cycle has the form shown in Fig. 6 and, of course, wastes gas. Here $2x_S$ is taken as 0.1 cm, and T_C is the total time the control acts during the cycle. For the 300-mile orbit, it is assumed that f_C can be no smaller than 10^{-2} cm/sec². This corresponds to a typical lower limit of 10^{-3} -lb thrust on a 100-lb vehicle.

It has been suggested a number of times to the author that the required thrusts would be much too small, or equivalently, the jet nozzle areas or chamber pressures required would be much too small to make cold gas jet control of a drag-free satellite feasible. This is not so. Commercial cold gas thrust systems are available "off-the-shelf" with thrusts in the 10^{-4} - to 10^{-2} -lb range and with rise and fall times on the order of a few milliseconds. The ratio T_C/T_D is equivalent to an effective thrust attenuation factor and is the basic reason why very small jets are not required. Thus, it is seen from Table 1 that the control requirements are reasonable.

Gas Consumed by a Nonideal Control System

In the examples shown, when the drag acceleration falls below one-tenth of its value at perigee, the jet for the left switching line begins to fire and gas is wasted. In general, it is impossible to avoid wasting some gas in high orbits since, as f_D approaches zero, the limit cycle becomes so long

that $\dot{x}_T - \dot{x}_B$ cannot be made small enough. It is instructive to compute an upper-bound on this wasted gas.

Let t_{DB} be the time in orbit after passing perigee at which the limit cycle begins to touch the left line, and assume that from time t_{DB} to time $T_O - t_{DB}$, f_D is exactly zero. Then

$$\frac{T_O - 2t_{DB}}{T_W} T_{CW} = \begin{matrix} \text{total time that thrust} \\ \text{is on during this period} \\ \text{of gas wasting} \end{matrix} \quad (30)$$

where

T_O = period of one orbit

T_W = period of one limit cycle while $f_D = 0$

T_{CW} = total time control is on during T_W

The weight of gas wasted per orbit is bounded by

$$\frac{W_{gw}}{\text{orbit}} \leq \frac{(T_O - 2t_{DB}) T_{CW}}{I_{sp} T_W} F_C \quad (31)$$

Equation (31) may be compared with the minimum possible gas used per orbit which is obtained from Fig. 4 using

$$W_{gmin}/\text{orbit} = W_{gtotal}(T_O/T_L) \quad (32)$$

The ratio $(W_{gw}/\text{orbit})/(W_{gmin}/\text{orbit})$ is given in Table 2 for an eccentricity of $e = 0.02$. The amount of wasted gas decreases monotonically as $\dot{x}_T - \dot{x}_B$ decreases.

In a practical satellite, the gas consumption rate must be multiplied by an additional factor that is never larger than $3^{1/2}$ because the control force must be resolved along three mutually perpendicular axes.

Finally, over the course of the lifetime of the satellite, some control gas will leak out, and this must be considered in the final lifetime calculation.

Translation Control without Attitude Control

If the vehicle has no attitude control, the control system is not as simple as that discussed in the previous section, but, on the other hand, it is not as complex as one might guess. This will be illustrated by considering a translation control system that uses linear time varying feedback.

In this section only, it will be convenient to view the vector r_C as a 3×1 column matrix denoted by r_C whose elements are the components of r_C resolved in a reference frame fixed in the satellite and to view $r_{C'}$ as a 3×1 column matrix whose elements are the components of r_C resolved in a nonrotating reference frame with its origin at the control center. \dot{r}_C or $\dot{r}_{C'}$ will simply mean the 3×1 column matrix whose elements are the time derivatives of the elements of r_C or $r_{C'}$ and will not imply from what frame vector differentiation is performed as was done with the dot and circle notation. Then r_C and $r_{C'}$ are related by the linear transformation

$$r_C = A r_{C'} \quad (33)$$

A is the direction cosine matrix connecting the two frames. In this notation, Eq. (6) becomes

$$\ddot{r}_C + 2\Omega \dot{r}_C + \dot{\Omega} r_C + \Omega^2 r_C = f_D + f_C \quad (34)$$

where

$$\Omega \triangleq \begin{pmatrix} 0 & -\omega_z & \omega_y \\ \omega_z & 0 & -\omega_x \\ -\omega_y & \omega_x & 0 \end{pmatrix} \quad (35)$$

is an antisymmetric matrix of angular velocities which yields the components of $\omega_S \times r$ when postmultiplied by r . By differentiating Eq. (33) and comparing the result with Eq. (43), it may be shown that $A = -PA$ and

$$A \dot{r}_{C'} = \dot{r}_C + \Omega A r_{C'} = r_C + \Omega r_C \quad (36)$$

If a control of the form

$$f_{C'} = -K_V \dot{r}_{C'} - K_P r_{C'} \quad (37)$$

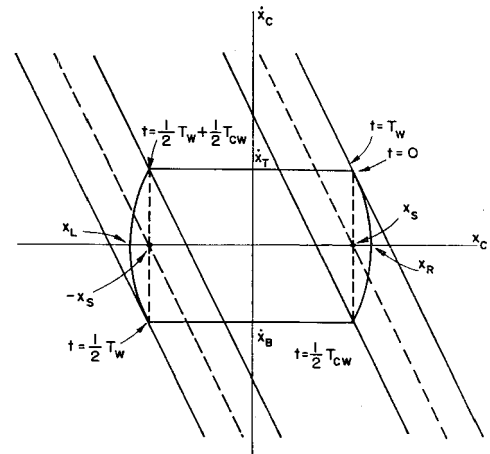


Fig. 6 Saturated limit cycle (typical numerical values are shown in the last line of each block in Table 1).

is selected for the nonrotating reference frame, K_V and K_P may be chosen to give any desired second-order performance:

$$\ddot{r}_{C'} = f_{D'} - K_V \dot{r}_{C'} - K_P r_{C'}$$

or

$$\ddot{r}_{C'} + K_V \dot{r}_{C'} + K_P r_{C'} = f_{D'} \quad (38)$$

gives the controlled equations of motion in the nonrotating reference frame. In the rotating reference frame (fixed in the vehicle),

$$f_C = A f_{C'} = -K_V A \dot{r}_{C'} - K_P A r_{C'} = -K_V (\dot{r}_C + \Omega r_C) - K_P r_C \quad (39)$$

or (in ordinary vector notation)

$$f_C = -K_V (\dot{r}_C + \omega_S \times r_C) - K_P r_C \quad (40)$$

Thus, in order to mechanize a linear translation control for arbitrary ω_S , it is only necessary to measure ω_S (for example with rate gyros) and to feed back Eq. (39) or (40). Then the controlled equation of motion written in a reference frame fixed in the satellite is

$$\ddot{r}_C + (K_V + 2\Omega) \dot{r}_C + (\Omega^2 + \dot{\Omega} + K_P + K_V \Omega) r_C = f_D \quad (41)$$

or (in ordinary vector notation)

$$\ddot{r}_C + (K_V + 2\omega_S \times) \dot{r}_C + [\omega_S \times (\omega_S \times) + \dot{\omega}_S \times + K_P + K_V \omega_S \times] r_C = f_D \quad (42)$$

Viewed in the light of all of Eqs. (41) and (42), the results of the previous section are obvious since (42) results from the transformation of the vector form of Eq. (38) by the Coriolis law

$$\dot{\cdot} = \dot{\cdot} + \omega_S \times \quad (43)$$

The control may be obtained then by merely separating out the terms that are multiplied by K_V or K_P in Eq. (42).

Thus, it is seen that, at least for the case of linear time varying feedback, complete absence of attitude control does not unduly complicate the mechanization of the drag-free satellite translation control.

Table 2 Typical upper-bounds on wasted gas for e = 0.02

h_P , statute miles	W_{gw}/orbit , lb	W_{gmin}/orbit , lb	W_{gw}/W_{gmin}
100	0.15	0.23	0.65
200	2.7×10^{-3}	8.2×10^{-3}	0.22
300	2.2×10^{-4}	7.6×10^{-4}	0.29

System Errors

Typical Translation Error Sources and Magnitudes

The terms F_{SB} and F_{PB} act on the ball and perturb its orbit, and extraneous torques act on a spinning rotor and cause it to precess. Each of these sources of error must be examined. F_{SB} is due to 1) gravitational attraction of the vehicle on the proof mass; 2) electromagnetic forces due to stray fields in the satellite and due to stray and induced charge and magnetic moment on the proof mass; 3) forces due to sensing the position of the proof mass (these can arise from optical radiation pressure or electric attraction from a capacitive pickoff); and 4) gas in the satellite cavity. F_{PB} can arise only from electromagnetic forces or possibly very energetic particle radiation, since the cavity physically isolates the proof mass from other outside disturbances.

If the control system acts to center the ball at a position where $F_{SB} + F_{PB} \neq 0$, the acceleration error of the satellite will be

$$f_{ss} + f_{PB} \triangleq f_{DB} \tag{44}$$

For ease of comparison, all translation error forces will be expressed in terms of their corresponding accelerations of the proof mass. The relative accelerations between the vehicle and the proof mass are unimportant except as they effect the mechanization of the control.

The sources and relative magnitudes of the various errors are summarized in Table 3. Typical numbers are computed for a drag-free satellite that could be used for a combined geodesy and aeronomy mission. The satellite and proof mass are assumed to have the following typical parameters: nominal satellite size, $2d = 0.61 \text{ m} = 2 \text{ ft}$; satellite mass, $m_s = 45.5 \text{ kg} = 3.12 \text{ slugs}$; satellite weight, $w_s = 445 \text{ newtons} = 100 \text{ lb}$; cavity radius, $d_1 = 3 \text{ cm}$; proof-mass radius, $R_B = 2 \text{ cm}$; proof-mass material, copper; proof-mass mass, $m_B = 0.30 \text{ kg}$; and proof-mass weight, $w_B = 2.9 \text{ newtons} = 0.66 \text{ lb}$. The derivations of the equations

in Table 3 and the underlying assumptions are explained in Appendix B.

Effect of Acceleration Errors on the Trajectory of a Drag-Free Satellite

Satellite trajectory equations

Although at first glance the trajectory equations of a drag-free satellite may appear to be quite complex, they are in fact rather simple. This is true because the control system constrains the satellite to follow the ball, and it is only necessary to consider Eq. (1), which describes the motion of the ball alone:

$$m_B \ddot{\mathbf{x}}_B = \mathbf{F}_{GB} + \mathbf{F}_{SB} + \mathbf{F}_{PB} \tag{45}$$

or

$$\ddot{\mathbf{x}}_B = \mathbf{f}_{GB} + \mathbf{f}_{SB} + \mathbf{f}_{PB} \tag{46}$$

If f_{SB} and f_{PB} were zero, the satellite motion would be that of a satellite acted on only by gravity, and the additional effect of f_{SB} and f_{PB} may be found by a perturbation analysis. The most convenient way to view the effects of f_{SB} and f_{PB} is to consider how much the actual trajectory deviates from the truly drag-free trajectory. Although it is not necessary, the analysis is greatly simplified if the actual motion is compared with a nominal circular orbit about a spherically symmetric earth. These linearized satellite equations were first written by Hill²³ in connection with his lunar theory and were applied to artificial satellites by Wheelon²⁴ and Geyling.²⁵ Their solutions are discussed in Refs. 24–28.

Linearized trajectory equations

Consider a locally level reference frame rotating about the ζ axis with its origin in a nominal circular orbit about a fixed gravitating center. Choose the ξ axis to be radially out from the attracting center, and the η axis parallel to the orbit velocity vector. Then the small amplitude linearized equations of motion of a satellite with respect to this reference frame are

Table 3 Error sources that disturb the orbit of the proof mass

Source of f_{SB} or f_{PB} disturbance	Relation	Key magnitudes	Typical values, acceleration in g_e 's
Vehicle gravity	$\frac{f}{g_e} = 0.7 \times 10^{-10} \left(\frac{r_{ZB}}{d_1} \right)$	$\frac{r_{ZB}}{d_1} = 0.1$	10^{-11a}
Leakage electric field in the cavity	$\frac{f}{g_e} = \frac{3 \epsilon_0 V_B E}{g_e \rho_m R_B^2}$	$V_B = 1 \text{ v}$ $q_B = 2.2 \times 10^{-12} \text{ coul}$ $E = 0.1 \text{ v/m}$	10^{-13}
Image attraction of spherical cavity for charged ball with zero stray field	$\frac{f}{g_e} = \frac{3 \epsilon_0 V_B^2}{g_e \rho_m R_B d_1^2} \left(\frac{r_Q}{d_1} \right)^3$	$\left(\frac{r_Q}{d_1} \right) = 0.1$	10^{-14}
Induced magnetic moment	$\mathbf{F} = (m_{HB} \cdot \nabla) \mathbf{H}$ $\frac{f}{g_e} = \frac{3 \chi_m m_{HS}^2}{4 \pi^2 \mu_0 d_1^3 \rho_m g_e}$	$\chi_m = 10^{-5}$ $m_{HS} / \mu_0 = 1 \text{ amp-m}^2$ $d = 0.2 \text{ m}$	10^{-12}
Motion through the earth's magnetic field ^b	$\frac{f}{g_e} = \frac{3 \epsilon_0 V_B v_O B_e}{g_e R_B^2 \rho_m}$...	10^{-13}
Electric force from capacitive pickup sensor	$\frac{f}{g_e} = \frac{\epsilon_0 A_C}{2 g_e m_B} \left(\frac{KC}{d_g \sigma_x} \right)^2 \left(\frac{\Delta d_g}{2 d_g} \right)$	See Appendix B	10^{-8a}
Radiation force from optical sensor	$\frac{W}{g_e} = \frac{W}{g_e m_{BC}}$	$W = 10^{-9} \text{ w}$	10^{-18}
Gas in the cavity	Not directly comparable but negligible	See discussion in Appendix B	...

^a These terms appear to be of the same order as the drag at very high altitudes; however, their effects are not of the same order since the drag always acts parallel to the velocity vector. See the section on the effects of the errors. Also, the large error due to a capacitive pickoff can be eliminated by using an optical pickup (see Appendix B).

^b This term is in fact zero inside a closed conducting cavity.

$$\begin{aligned} \ddot{\xi} - 3\omega_0^2\xi - 2\omega_0\dot{\eta} &= f_{DB\xi} \\ 2\omega_0\dot{\xi} + \ddot{\eta} &= f_{DB\eta} \\ \ddot{\zeta} + \omega_0^2\zeta &= f_{DB\zeta} \end{aligned} \tag{47}$$

In deriving these equations, terms are neglected which are equivalent to dropping terms in e^2 and higher, and, thus, they are quite accurate for orbits with $e < 0.1$ and are reasonably good for values of e up to 0.3. In addition, ξ and η may be interpreted as either rectangular or polar coordinates (where η is "wrapped around" the nominal orbit). The rectangular coordinate interpretation is valid for ξ and η small and for $\dot{\xi}$ and $\dot{\eta}$ arbitrary, and the polar coordinate interpretation is valid for $\xi, \dot{\xi}$, and $\dot{\eta}$ small and η arbitrary.²⁷

Types of disturbing acceleration

It is convenient to divide the disturbing accelerations into two classes: 1) nonrotating with respect to the ξ, η frame and 2) nonrotating with respect to an inertial frame. When Eq. (47) is solved, the dominant secular terms for case 1 are

$$\xi = f_{DB\eta}t/\omega_0 \tag{48}$$

$$\eta = -\frac{3}{2}f_{DB\eta}t^2 \tag{49}$$

and for case 2 they are

$$\xi = \frac{3}{2}(f_{DB\zeta}/\omega_0) \sin\omega_0 t \tag{50}$$

$$\eta = 3(f_{DB\zeta}/\omega_0)(1 + \cos\omega_0 t) \tag{51}$$

These equations represent the deviations along ξ and η caused by f_{DB} . As a numerical example, if $f_{DB} = 10^{-11}g_e \approx 10^{-10}$ m/sec², $t = 1$ yr $\approx 3 \times 10^7$ sec and $\omega_0 \approx 10^{-3}$ rad/sec; then $f_{DB}t^2 \approx 10^5$ m $\approx 300,000$ ft ≈ 60 miles and $f_{DB}t/\omega_0 = 3$ m ≈ 10 ft.^{**} The solution of the third of Eqs. (47) does not have any secular terms for constant $f_{DB\zeta}$, and it is necessary to consider the next higher term, which is nonlinear. This equation is given by

$$\ddot{\zeta} + \omega_0^2\zeta = 3\omega_0^2(\xi\zeta/a) + f_{DB\zeta} \tag{52}$$

$$\zeta = -(3e/2)(f_{DB\zeta}t/\omega_0) \cos\omega_0 t \tag{53}$$

which corresponds to a slow rotation of the orbit plane at a rate $3e/2\omega_0 a$.^{††} Using these results, it is possible to estimate the effect of the acceleration errors listed in Table 3 for various types of missions. These missions are most conveniently characterized in terms of their attitude control when comparing the various disturbances.

^{**} The length of time for which the results of the linear perturbation analysis may be safely extrapolated depends on the effects of the nonlinear terms that have been neglected. These neglected terms will, in general, give rise to terms in the solution containing powers of $e\omega_0 t$, and they may be neglected if $e\omega_0 t \ll 1$. For an exactly circular orbit, e remains less than 10^{-6} for the case of Eqs. (50) and (51); and a 1-yr extrapolation appears reasonable. The results implied by the circular-orbit linear analysis are not valid for one year, however, if the initial conditions correspond to eccentricities of the order of 0.01. This does not imply that the results of this section are incorrect for eccentricities of this order, but merely that they do not follow from the previous considerations. If the satellite equations are linearized about a nominal elliptical orbit (linear form of Encke's method) and integrated numerically for 1 orbit period, the periodic part of the fundamental matrix may be factored from the part that grows with time, and the effect of the perturbations for one year may be computed. When this is done, it is now Ae that remains less than 10^{-6} , and the neglected terms are not significant. The results of this type of analysis are essentially the same as the circular-orbit calculations.

^{††} This solution is, of course, also only the first term of a power series in t and is valid for only a limited time. When considering the case of a spinning satellite, it will be assumed that the satellite spin vector is occasionally realigned normal to the orbit by the attitude control so that Eq. (54) is valid for all time.

Satellite attitude controlled to a locally level reference frame

When the satellite attitude control system keeps the vehicle locally level, the disturbances do not rotate in the ζ, η frame, and the results of case 1 apply. Since a sizable component of the disturbance is almost certain to appear along η , this is clearly the worst case and can result in very large deviations.

Satellite attitude controlled to an inertially nonrotating reference frame (gyroscope experiments)

Here case 2 applies, and the departures from the nominal can probably be limited to only a few meters per year except when a capacitive pickup is used. In that case, errors as large as several kilometers might develop in a year. If, however, the mission is primarily to make gyrodrift measurements, the trajectory errors are not important.

Satellite spinning with the spin normal to the orbit plane (geodesy and aeronomy missions)

If the satellite spins with an angular velocity held normal to the orbit plane that is large in comparison with ω_0 , the effects of those forces, which are fixed in the satellite and which are not modulated at the spin rate, average to zero except along the spin axis.

Examples of forces which do not average to zero are provided by any force whose magnitude depends on the ball's position relative to the satellite (since r_{SC} will not be zero and the force will be modulated at the satellite spin rate) and by the force due to the motion of a charged ball through the earth's magnetic field and the electric image attraction force (which are not fixed in the satellite). Nevertheless, with the exception of the capacitive pickup (which can be replaced with an optical pickup) and the nonspinning forces (which are small), the effect of the dominant other disturbing acceleration due to vehicle gravity can be attenuated either by a factor of e [since Eq. (53) applies when the spin is normal to the orbit^{††}] or by a factor equal to the percent modulation of the gravitational force at spin frequency (whichever is larger) by spinning the satellite with the spin vector normal to the orbit plane.

Under the foregoing circumstances, the departure of the satellite from an orbit, which would be caused by gravity alone, could possibly be limited to only 1 m/yr or so, and this would truly be a drag-free satellite.

Gyroscope Random Drift

The sources and magnitudes of the various torques that can cause random drift rates are summarized in Table 4. Typical numbers are computed for a spherical rotor with the following parameters: material, silicon; radius (R_B), 2 cm; mass (m_B), 80 g; moment of inertia (C), 128 g-cm² = 1.28×10^{-5} kg-m²; spin rate (ω_B), 10^3 rad/sec $\approx 10^4$ rpm; angular momentum (h_B), 1.28×10^5 dyne-cm-sec = 1.28×10^{-2} newtons-m-sec; and sphericity factors ϵ_1 and ϵ_2 , 10^{-5} .

The derivation of the formulas in Table 4 and their underlying assumptions are explained in Appendix C. ϵ_1 and ϵ_2 are dimensionless parameters that are used to estimate the effects of the lack of sphericity of the rotor and are also discussed in Appendix C.

The results of the calculations summarized in Table 4 indicate that it may be possible to build a gyroscope whose random drift rate is less than 0.1 sec-arc/yr. This represents an improvement of about five or six orders of magnitude over the best current instruments. The possibility of achieving such performance should admittedly be accepted with some skepticism; however, one of the very important uses of the drag-free satellite would be to test the results in Table 4. These tests would be important, not so much be-

^{††} It should be noted that the accuracy of this alignment need only be maintained to a factor of e .

cause one might ever want to build operational drag-free satellite inertial systems (although this might be the case), but because the effects listed in Table 4 will ultimately limit the performance of any gyroscope that could be built. In addition, even if a gyroscope in a satellite is supported instead of floating free, the drag accelerations are so small that performance can approach the numbers listed in Table 4, and it is clear that a whole new class of gyroscopes could be developed for satellite applications. The drag-free satellite can act as a research vehicle that will allow these results to be known years before it would otherwise be possible.

Gyroscope Readout

One of the most difficult questions, and one that is not discussed in this paper, is the spin or angular momentum vector readout technique. Stanford University, Minneapolis-Honeywell, and the University of Illinois are all working on feasible readout schemes. It is felt by the author that any description of the details of the various systems should be given by these groups. It does appear, however, that readout to this order of accuracy is quite possible and that it can be done without causing excessive drift rates.

One complication that arises when one tries to read the direction of the angular momentum vector of an almost isoinertial gyrorotor is that the preferred axis of rotation (i.e., the axis of maximum moment of inertia) is difficult to identify in

advance. This means that readout schemes that depend on body-fixed patterns are not quite as useful as they are on rotors where one axis of inertia is much larger than the other two. This is true because the angular velocity vector may move a considerable distance in the rotor body-fixed axis if the spin is not started parallel to the preferred axis. For an almost spherical rotor with principal moments of inertia $A = C(1 - \epsilon_1)$, $B = C(1 - \epsilon_2)$, and C (where ϵ_1 and ϵ_2 are of the order of 10^{-5}); it can be shown that the angle ψ between the angular momentum vector and the angular velocity vector is given by

$$\psi = \left[\epsilon_1^2 \left(\frac{\sin 2\alpha}{2} \right)^2 + \epsilon_2^2 \left(\frac{\sin 2\beta}{2} \right)^2 - 2\epsilon_1\epsilon_2 \cos^2\alpha \cos^2\beta \right]^{1/2}$$

and

$$\psi = \epsilon_1 \frac{\sin 2\gamma}{2} \quad \text{if} \quad \epsilon_1 = \epsilon \quad (54)$$

α , β , and γ are the respective angles from the rotor x_B , y_B , and z_B principle axes to the angular velocity vector. ψ has a maximum value of the order of ϵ_1 or ϵ_2 , and, when viewed from an inertial reference frame, the angular velocity vector rotates about the angular momentum vector at a rate that is practically equal to the angular velocity. If ϵ_1 and ϵ_2 are of the order of 10^{-5} , it would appear that any readout that does not have a response time faster than $2\pi/\omega_B$ will tend

Table 4 Unsupported gyrodrift rates (1 sec-arc/yr = 3.18×10^{-8} deg/hr = 1.5×10^{-13} rad/sec)

Source of torque	Formula for $\dot{\phi}_{\text{peak}}$	Key assumptions and magnitudes	Typical drift rates (rad/sec)
Gravity gradient	$\frac{3\omega\omega^2}{2\omega_B}$	$\epsilon = 10^{-5}$; $\omega_B = 103$ rad/sec	5×10^{-14}
Magnetic eddy currents	$\frac{B_{\perp} B \ \sigma\ }{4\rho_m}$	$B = 2 \times 10^{-5}$ webers/m ² $\sigma = 10$ mho/m	4×10^{-13a}
Barnett effect	$\frac{5\chi_m H}{\rho_m R_B^2 (e/m) g_H}$	$H = 25$ amp turns/m $g_H = 2$, $\chi_m = 10^{-5}$	10^{-15}
Einstein-de Haas	$\frac{5\chi_m \dot{H}}{\rho_m R_B^2 (e/m) g_H \omega_B}$	\dot{H} only due to motion through earth's field	10^{-21}
Spinning charge	$\frac{15\epsilon_0 V_B B}{4\rho_m R_B^2}$	$V_B = 1$ v	7×10^{-16}
Tolman effect	Neglected on the grounds that it is smaller than spinning charge		
Induced magnetic moment in an ellipsoid	$\frac{\chi_m^2 B_0' H_0'' \epsilon}{\rho_m R_B^2 \omega_B}$...	10^{-21}
Induced magnetic moment in single crystal	$\frac{5B_0' H_0'' (\chi_m'' - \chi_m')}{2\rho_m R_B^2 \omega_B}$	$\chi_m'' - \chi_m' = 10^{-6}$	10^{-12b}
Impurity ferromagnetism	Neglected on the grounds that experimenters could not have obtained accurate values of χ_m if this were important.		
Electric moment induced in ellipsoid by nonuniform electric field	$\frac{15}{4} \frac{\epsilon_0 E_{\text{max}}^2 \epsilon}{\rho_m R_B^2 \omega_B}$	$E_{\text{max}} = 0.1$ v/m	3×10^{-21}
Charge on the ellipsoid plus leakage field	$\frac{15\epsilon_0 V_B E_{\text{max}} \epsilon}{2\rho_m R_B^3 \omega_B}$		7×10^{-18}
Charge on the ellipsoid plus image field	$\frac{15\epsilon_0 V_B^2 \epsilon}{2\rho_m R_B^2 d_1^2 \omega_B} \left(\frac{r_Q}{d_1} \right)^3$	$\frac{r_Q}{d_1} = 0.1$	10^{-18}
Surface electric eddy currents in an ellipsoid (power dissipation)	$\frac{15\epsilon_0^2 V_B^2 c^2}{2l_i \rho_m R_B^3 \sigma}$	$l_i = 10^{-10}$ m	3×10^{-21}
Surface electric eddy currents (magnetic moment)	$\frac{15\epsilon_0 V_B B \epsilon}{4\rho_m R_B^2}$...	7×10^{-21}
Sensor radiation pressure	$\frac{15 W}{8\pi \rho_m R_B^4 c \omega_B}$	$W = 10^{-9}$ w	5×10^{-18}
Gas in cavity	$\langle \phi^2 \rangle_{\text{av}} = \frac{2bkT}{\hbar B^2} t$ $b = \frac{\pi}{9} R_B^4 \rho \left(\frac{3kT}{m_{\text{av}}} \right)^{1/2}$	$T = 300^\circ\text{K}$	$\langle \phi^2 \rangle_{\text{av}}^{1/2} = 5 \times 10^{-13}$ rad in 1 yr

^a This number may be reduced to 4×10^{-15} by a magnetic shield with an attenuation factor of 0.1 which is easily attained.

^b In polycrystalline silicon this effect will be much smaller, and it may also be reduced by magnetic shielding.

to read the average direction of ω_B which, of course, is the direction of the angular momentum. Thus it seems at the present time that sufficiently accurate readout schemes can be developed. Further details on this subject will have to await papers by the forementioned groups.

Conclusion

It has been shown that there appears to be no fundamental physical or engineering reason why a drag-free satellite cannot be built at this time. Such a vehicle would yield useful immediate results in geodesy and aeronomy and would lay the foundations for the construction of very good gyroscopes and possibly open the way to do the Pugh-Schiff relativity experiment. In addition, the actual mechanization of the translation control would not be overly complex. For simple vehicles, no attitude control is necessary since three rate gyros will give sufficient attitude information to implement the control. The jet thrust levels and attainable fuel lifetimes are quite reasonable and should cause no difficulty.

A spinning drag-free satellite with its spin vector normal to the orbit plane and with an optical position sensor would depart from a purely gravitational orbit by only 1 m/yr. Distances this small cannot be detected by any present or foreseeable tracking apparatus, and such performance would be drag-free in every practical sense.

Appendix A : Translation Control Equations—Special Cases

Three-Axis Attitude Control to an Inertial Reference

If the drag-free satellite possessed perfect attitude control to an inertial reference, ω_S and O_S would be identically zero, and Eq. (6) would become

$$m_B \ddot{\mathbf{r}}_C = \Delta \mathbf{F}_G + \left(1 + \frac{m_B}{m_S}\right) \mathbf{F}_{SB} + \left(\mathbf{F}_{PB} - \frac{m_B}{m_S} \mathbf{F}_{PS}\right) - \frac{m_B}{m_S} \mathbf{F}_{CS} \quad (A1)$$

Equation (A1) then reduces to three uncoupled equations of the form

$$\ddot{x}_C = \frac{1}{m_B} \left[\Delta F_{Gx} + \left(1 + \frac{m_B}{m_S}\right) F_{SBx} + \left(F_{PBx} - \frac{m_B}{m_S} F_{PSx}\right) \right] - \frac{F_{CSx}}{m_S} \quad (A2)$$

$$\triangleq f_{Dx} + f_{Cx}$$

where the drag is the dominant source of f_D .

In order for these equations to be valid, the attitude control must act such that the neglected terms are much smaller than $\ddot{\mathbf{r}}_C$. To investigate the conditions under which this is true, assume for simplicity that linear constant coefficient feedback control systems act such that the translation and attitude responses are second-order and critically damped with time constants T_r and T_θ , respectively. Then it turns out that the foregoing requirement will be satisfied if $T_\omega \geq T_r$ and if an equivalent impulsive disturbance in attitude θ_{max} satisfies

$$\theta_{max} \ll (1/T_r) \quad (A3)$$

The control associated with the plant represented by Eq. (A2) is discussed in the second section in order to illustrate the basic problems; but, in general, it is more convenient (and for geodetic missions more desirable) not to control attitude at all.

Constant Spin about a Preferred Axis

If the satellite is symmetric such that $I_1 = I_2 \neq I_3$, and if the satellite is stably oriented with respect to the orbit

plane,²⁹ and if the other disturbing torques are negligible, then $\omega_S = \omega_z$ is constant and Eq. (6) is

$$\ddot{\mathbf{r}}_C + 2\omega_S \times \dot{\mathbf{r}}_C + \omega_S \times (O_S \times \mathbf{r}_C) = \mathbf{f}_D + \mathbf{f}_C \quad (A4)$$

In a reference frame with the z axis parallel to the spin axis, (A4) becomes

$$\begin{aligned} \ddot{x}_C - \omega_S^2 x_C - 2\omega_S \dot{y}_C &= f_{Dx} + f_{Cx} + 2\omega_S \dot{x}_C + \\ \ddot{y}_C - \omega_S^2 y_C &= f_{Dy} + f_{Cy} \quad (A5) \\ \ddot{z}_C &= f_{Dz} + f_{Cz} \end{aligned}$$

Attitude Uncontrolled (i.e., Arbitrary Spin)

For

$$\omega = \begin{pmatrix} \omega_x \\ \omega_y \\ \omega_z \end{pmatrix} \quad (A6)$$

Omitting the subscript C , Eq. (6) becomes

$$\left. \begin{aligned} \ddot{x} - (\omega_y^2 + \omega_z^2)x - 2\omega_z \dot{y} + (\omega_x \omega_y - \dot{\omega}_z)y + \\ 2\omega_y \dot{z} + (\omega_x \omega_z + \dot{\omega}_y)z &= f_{Dx} + f_{Cx} \\ 2\omega_z \dot{x} + (\omega_y \omega_x + \dot{\omega}_z)x + \ddot{y} - (\omega_x^2 + \omega_z^2)y - \\ 2\omega_x \dot{z} + (\omega_y \omega_z - \dot{\omega}_x)z &= f_{Dy} + f_{Cy} \\ -2\omega_y \dot{x} + (\omega_z \omega_x - \dot{\omega}_y)x + 2\omega_x \dot{y} + (\omega_z \omega_y + \dot{\omega}_x)y + \\ \ddot{z} - (\omega_x^2 + \omega_y^2)z &= f_{Dz} + f_{Cz} \end{aligned} \right\} \quad (A7)$$

Appendix B: f_{SB} and f_{PB} Error Sources

Errors Due to Vehicle Gravity

In the vehicle there is a set of points which may be called the points of zero self-gravity or ZSG points. They have the following properties:

- 1) The ZSG points are fixed in a rigid body, and they are not the same as the center of mass or the center of gravity.
- 2) In a region of free space, a ZSG point is a saddle point or a neutral point of the potential energy. This follows by examining the proof of Earnshaw's theorem (see Jeans³⁰).
- 3) The ZSG is not a unique point but may be a finite number of points, a countably infinite number of points, or an uncountably infinite number. This is evident from the following simple examples: three point masses in a line, a dumbbell with solid spheres on each end, a line mass ring, two coaxial line mass rings, a circular cylindrical shell, a hollow cylindrical body with wall of finite thickness, or a solid cylinder.
- 4) A ZSG point is located at the center of mass of a body if $\rho_m(\mathbf{r}) = \rho_m(-\mathbf{r})$. In the neighborhood of a ZSG point, the acceleration error from the vehicle gravity is

$$f_{BVG} = K(Gm_S/d^2)(r_{zB}/d) \quad (B1)$$

where

$$r_{zB} = |\mathbf{r}_C - \mathbf{r}_{Cz}| \quad (B2)$$

d is a distance that is characteristic of the vehicle size, and K is a numerical factor that depends on the vehicle geometry. For example, in a hollow uniform spherical shell, $K = 0$; and, in a solid homogeneous sphere of radius d , the factor $K = 1$. To obtain a rough estimate of the value that K might reasonably be expected to assume, consider a homogeneous circular cylindrical body of inner radius d_1 , outer radius d_2 , and height $2h_s$. The second term in the series expansion of the potential at the center is given by

$$\phi_2 = -K_2(Gm_S/d_1)(r_{zB}/d_1)^2 P_2 \quad (B3)$$

where

$$K_2 = \left\{ \frac{[1 + (h_s^2/d_1^2)]^{-1/2} - [(d_2^2/d_1^2) + (h_s^2/d_1^2)]^{-1/2}}{(d_2^2/d_1^2) - 1} \right\} \quad (B4)$$

and P_2 is the second Legendre polynomial. If, for example, $d_1 = 0.1$ ft, $d_2 = 1$ ft, and $h_s = 1$ ft, then $K_2 = 1/344$. If $r_{ZB} = d_1$, the term ϕ_2 adequately represents the potential, and

$$\left. \begin{aligned} f_{BVG} &= -(\partial\phi_2/\partial r) = -2K_2(Gm_s/d_1^2)(r_{ZB}/d_1)P_2 \\ f_{BVG \max} &= -2K_2(Gm_s/d_1^2)(r_{ZB}/d_1) \\ f_{BVG \max}/g_e &\approx 0.7 \times 10^{-10} (r_{ZB}/d_1) \end{aligned} \right\} \quad (B5)$$

if $g_e m_s = 100$ lb.

The control system can easily keep the average value of r_C to 1 mm or less, but the error in centering the control center on a ZSG point could be of the order of 1 cm. In addition to this, the ZSG point will shift as gas is expelled unless the location of the gas tanks is symmetrical to this point. Thus, under these conditions, $f_{BVG \max}/g_e$ would be of the order of 10^{-11} . There are only two possible ways to find the location of the central ZSG point in the satellite. It can either be calculated from a knowledge of the mass position of each component in the satellite structure and equipment, or it might be measured with some device such as a torsion balance after the satellite is constructed. Both of these approaches present great difficulties, but they do not appear insurmountable. If, for example, the effect of a 10-g mass located 10 cm from the central ZSG point were neglected in the computation, this would cause an error of about 10^{-8} cm/sec² of about $10^{-11} g_e$. This is equivalent to a 4.2-mm error in locating the ZSG point.

Errors Due to Electric and Magnetic Fields

If the ball collects a small unknown residual charge, any stray electric field will apply an unknown force to it. In addition, if the ball is located in a shielded metal cavity, the charge on the ball would be attracted to induced charges on the cavity walls. A conducting ball inside a completely enclosed metal cavity could be discharged merely by contacting the walls. The charge on the ball would be exactly zero, and the static field inside the cavity would be exactly zero. This is true even for a shield of finite conductivity. It is not possible, however, to construct a completely enclosed cavity because the position of the ball must be sensed. Furthermore, for some applications, a nonconducting or even a transparent ball might be desirable; and, therefore, it is instructive to compute the minimum charge on the ball which could be measured and the minimum electric field in the cavity which could be detected.

Maximum charge that might reasonably be expected to accumulate on the proof mass

The primary mechanisms for charging the proof mass will be due to the differences in the average velocities of electrons and ions from ionized air molecules and to the photoelectric effect from cavity illumination. At 400-km altitude, a large fraction of the air molecules are ionized, and the kinetic temperature is about 1000°K, but, on the inside of the satellite cavity, collisions with the walls should quickly discharge the ions and reduce their kinetic temperature to that of the satellite (about 300°K). Even if as many as half the gas molecules were ionized, the ball would probably not accumulate a negative charge much greater than 1 v.

W. M. Fairbank of Stanford University has suggested to the author that, if the proof mass and the cavity walls are both coated with a photoelectric material and if the cavity is weakly illuminated with a radiation whose wave/length is chosen to give a stopping potential of about 0.1 v or less, then the potential on the proof mass will assume an equilibrium value of 0.1 v or less. Thus it will be assumed that, by this or some similar technique, the charge on the proof mass can be limited to no more than 1 v, which corresponds to a charge of $q_B = 4\pi\epsilon_0 \times 1 \text{ v} \times 0.02 \text{ m} = 2.2 \times 10^{-12}$ coul $\approx 10^{+7}$ electrons.

Maximum electric field that can leak into the cavity

The question of what stray electric fields other than those due to a charge on the proof mass might be present in the cavity can be answered in the following way. If the proof mass were uncharged and if the cavity walls were a completely closed conductor, there could be no static electric field present. As a practical matter, however, the cavity walls will need to have small holes in them to accommodate the position sensing apparatus, and any charge that has accumulated on the outside of the satellite will cause a residual electric field to leak through these holes. Furthermore, the accumulated charge on the outside of the satellite may be fairly large, corresponding to a potential of several (or in a few cases several hundred) volts.

If a closed conducting charged shell has an electric field E_n at some point on its surface, then there will be a field $E_n/2$ at this same point if a small hole is drilled there. Gauss's law implies that the charge that is then inside the closed conductor is given by

$$q_{\text{inside}} = \frac{1}{2} \frac{A_{\text{hole}}}{A_{\text{surface}}} q_{\text{outside}} \quad (B6)$$

The electric field on the inside will depend on how the inner charge is distributed, but generally it will be concentrated near the hole. If additional shields are used, each one will attenuate the charge according to Eq. (B6). For the purpose of a simple computation, it will be assumed that the static electric field can be limited to less than 0.1 v/m inside of the cavity containing the proof mass by a series of concentric shielded cavities or, equivalently, by bringing in leads or light beams through tubes whose lengths are big compared to their diameters.

Force on a charged ball due to leakage electric field

A stray electric field of 0.1 v/m would cause an error acceleration on a 300-g ball with a charge of 2.2×10^{-12} coul which is given by

$$\frac{f}{g_e} = \frac{q_B E}{g_e m_B} = \frac{3\epsilon_0 V_B E}{g_e \rho_m R_B^2} \approx 10^{-13} \quad (B7)$$

Force on a charged ball due to image attraction with zero leakage field

For a spherical cavity of radius d_1 , the force on a point charge inside the cavity is given by

$$\frac{f}{g_e} = \frac{q^2}{4\pi\epsilon_0 d_1^2 g_e m_B} \left(\frac{r_Q}{d_1}\right)^3 \left[1 - \left(\frac{r_Q}{d_1}\right)^2\right]^{-1} \approx \frac{3\epsilon_0 V_B^2}{g_e \rho_m R_B d_1^2} \left(\frac{r_Q}{d_1}\right)^3 \quad (B8)$$

where r_Q is the distance of the point charge from the equilibrium point at the center. The acceleration that corresponds to this for a 3-cm radius cavity and a potential of 1 v and a position error of 0.3 cm is

$$f/g_e = 10^{-14} \quad (B9)$$

Magnetic force due to field gradients

The force on the ball due to stray magnetic fields is

$$\mathbf{F} = (\mathbf{m}_{HB} \cdot \nabla) \mathbf{H} \quad (B10)$$

If the ball is constructed of nonferromagnetic materials, there will be no residual magnetic moment, and the only source of \mathbf{m}_{HB} is a moment induced by the stray magnetic field.

Stray magnetic fields can arise from two sources, those in the satellite and those external to the satellite. The external field primarily will be due to the earth's magnetism and is of the order of 2×10^{-5} webers/m². Magnetic fields in the satellite arise from current loops, ferromagnetism, and unexplained residual magnetic moments. Bandeen and Man-

ger³¹ report apparent residual values of m_{HS}/μ_0 of 1 amp-m² in Tyros I, and this is considerably larger than the magnetic moment expected from the electrical circuitry and is probably the largest value one might expect. The magnetic field in the satellite which corresponds to a magnetic moment of this size is of the order of the earth's field. However, its gradient is much larger than the gradient of the earth's field, and, hence, it can exert a much larger force on the ball. The maximum acceleration of the ball due to a residual magnetic moment m_{HS}/μ_0 of 1 amp-m² located in the satellite a distance $d = 0.2$ m from the ball as computed from (B10) is

$$J_{B \max} = \frac{3\chi_m m_{HS}^2}{4\pi^2 \mu_0 d^3 \rho_m} \approx 10^{-12} g_e \quad (B11)$$

Force due to the motion of a charged ball through the earth's field

Since the charge on the ball is in motion through the earth's magnetic field, this field exerts a force on the ball given by

$$\mathbf{F}_{PB} = q \mathbf{v}_O \times \mathbf{B}_e \quad (B12)$$

For a 300-g ball with a stray charge of 2.2×10^{-12} coul, this corresponds to an acceleration

$$\frac{f}{g_e} = \frac{3\epsilon_0 V_B v_O B_e}{g_e R_B^2 \rho_m} \approx 10^{-13} \quad (B13)$$

The magnitude of this effect is computed for illustrative purposes only, since it is actually zero inside of a closed conducting cavity.

Errors Due to Sensing the Position of the Proof Mass

Capacitive pickup position sensor

If a capacitive pickup is used, it will exert an electric pressure on the ball given by $\epsilon_0 E_n^2/2$. The electric field is proportional to the input voltage to the position circuitry, and the input voltage required depends on the precision with which the position of the ball must be resolved. Since the velocity of the ball with respect to the satellite can be inferred only from the position measurements, the minimum tolerable velocity error determines the necessary precision of the position measurements. Typical values for the minimum velocity error may be obtained from Table 1. The worst case in the table occurs at 300 miles where a velocity measurement to the order of 10^{-3} cm/sec is necessary to mechanize the control. It is assumed that the position measurement errors can be represented by white noise that is averaged by a single time constant filter with time constant $T_1 = 2\pi/\omega_1$. It is further assumed that the velocity is formed by a filter of the form

$$H(j\omega) = \frac{j\omega}{j\omega/\omega_2 + 1} \quad (B14)$$

so that the velocity error is given in terms of the position error by

$$\sigma_v = \sigma_x \left(\frac{\omega_1 \omega_2^2}{\omega_1 + \omega_2} \right)^{1/2} = \sigma_x \left(\frac{\omega_1}{2^{1/2}} \right) \quad (B15)$$

if $\omega_1 = \omega_2$. Alternately,

$$\sigma_x = [(2)^{1/2} T_1 / 2\pi] \sigma_v = 0.225 T_1 \sigma_v \quad (B16)$$

Thus, to limit the velocity error to 10^{-13} cm/sec, the position must be measured to 2.25×10^{-5} cm if $T_1 = 100$ msec. If it is assumed that with a 100-v input to the capacitive circuitry the pickup can resolve 10^{-4} times the nominal gap width, then it is possible to compute the force from the electric pressure. A typical capacitive pickup would use a set of input plates to couple the input voltage to the ball and three

pairs of output plates to read position in each axis. The computation of the force on the ball is rather involved, but, if the departure from equilibrium is small, it may be approximated by

$$\frac{f}{g_e} = \frac{\epsilon_0 A_C}{2g_e m_B} \left(\frac{V_C}{d_g} \right)^2 \left(\frac{\Delta d_g}{2d_g} \right) \quad (B17)$$

where d_g is the nominal gap width and A_C is the area of the plates. If $A_C = 1$ cm², $d_g = 0.2$ cm, and $\Delta d_g/2d_g = 0.1$, then

$$f/g_e \approx 3.76 \times 10^{-12} V_C^2 (V_C \text{ in volts rms}) \quad (B18)$$

If it is further assumed that the measurement noise is additive with zero mean and uncorrelated with position, then V_C and σ_x are related by an expression of the form

$$V_C = K_C / \sigma_x \quad (B19)$$

From Eq. (B16) and the previous assumption of the pickup sensitivity, $K_C = 0.1$ v-cm/sec. Thus

$$\frac{f}{g_e} \approx \frac{\epsilon_0 A_C}{2g_e m_B} \left(\frac{K_C}{d_g \sigma_x} \right)^2 \left(\frac{\Delta d_g}{2d_g} \right) \quad (B20)$$

$$\approx \frac{3.76 \times 10^{-14} \text{ cm}^2/\text{sec}^2}{\sigma_x^2} \quad (B21)$$

For a given altitude, the value of σ_x which can be tolerated may be inferred from Table 1 and is of the order of 10^{-2} cm/sec for $h_P = 100$ miles and 10^{-3} cm/sec for $h_P = 200$ or 300 miles. It follows that

$$f_{SB}/g_e \approx 4 \times 10^{-10} \text{ for } h_P = 100 \text{ miles} \quad (B22)$$

$$f_{SB}/g_e \approx 4 \times 10^{-8} \text{ for } h_P = 200 \text{ or } 300 \text{ miles}$$

For a 300-mile orbit, a capacitive pickup will provide about as much disturbance as the drag on the vehicle; and, for missions in this altitude range or for any mission where the capacitive pickup causes disturbances that are too large, it will be necessary to use an optical pickup. On the other hand, for aeronomy or geodetic missions where h_P is less than 200 miles, a capacitive pickup may be quite satisfactory.

Optical position sensor

One arrangement that could sense the position of the ball would use a single light source and a single photomultiplier tube. The light from the source is chopped by a vibrating reed or a linear electro-optical device, and then with the aid of fixed mirrors it is split into six rectangular beams, two for each axis. The chopper acts such that only one beam at a time is on, so that the output signal is time shared among the beams. To measure displacement on a given axis, the beams are aimed such that, when the ball is in its centered position, it intercepts about half of each beam and such that displacement along that axis covers one beam and uncovers the other. The signals from beams on opposite sides of the ball are subtracted, and this difference signal is proportional to the deviation of the ball from its centered position.

It is necessary to use a single light source and a single photomultiplier to reduce the effects of drift, and it is necessary to chop the light source in order to distinguish the beams (by time sharing), avoid the drift problems inherent in d.c. amplifiers, and to prevent the encoding of low-frequency noise on the signal.

The minimum change in position which can be detected depends on the photomultiplier noise properties. Engstrom³² quotes minimum detectable powers of 10^{-14} w with a bandwidth of 1.8 cps for photomultiplier tubes. For a bandwidth of 10 cps this corresponds to approximately 5×10^{-14} w. The position error σ_x is given by

$$\sigma_x = N d_b / 2W \quad (B23)$$

where d_b is the width of the beam, W the power in the beam, and N the noise equivalent power of the phototube. For example, if $N = 5 \times 10^{-14}$ w, $\mathbf{g} = 4$ mm, and $W = 10^{-9}$ w,

$$\mathbf{a}_r \approx 10^{-5} \text{ cm} \quad (\text{B24})$$

The disturbing force (which is due to radiative pressure) is given by

$$F = W/c$$

$$f/g_e = (W/g_e m_B c) \approx 10^{-18}$$

Thus, for those applications where the capacitive pickup would disturb the ball excessively, the use of an optical pickup can reduce the disturbance by nine or ten orders of magnitude.

Brownian Motion of the Proof Mass

The effect of gas in the cavity can be divided into two parts, a macroscopic resistive force proportional to the velocity and a microscopic force noise with zero mean that is due to individual molecular collisions. This division of effect is to some extent arbitrary, but it has proved quite successful in the classical theory of Brownian motion of colloidal particles. This gives the equation of motion

$$\ddot{x}_C + (p/m_B)\dot{x}_C = f_{D_{\text{gas}}} \quad (\text{B26})$$

If the molecular force noise is considered to be white and if it is assumed that equipartition of energy eventually obtains, then Eq. (B26) may be integrated by the technique described in Aseltine³³ and Kennard.³⁴ For zero initial conditions at $t = 0$,

$$\langle \dot{x}_C^2 \rangle_{\text{av}} = (kT/m_B)(1 - e^{-2pt/m_B}) \quad (\text{B27})$$

$$\langle x_C^2 \rangle_{\text{av}} = \frac{2kT}{p} \left[t - \frac{2m_B}{p} (1 - e^{-pt/m_B}) + \frac{m_B}{2p} (1 - e^{-2pt/m_B}) \right] \quad (\text{B28})$$

p depends on the surface properties of the sphere and may be evaluated from kinetic theory. For an order of magnitude estimate, it will be taken as

$$p = 6\rho A_B \left(\frac{kT}{2\pi m_{\text{av}}} \right)^{1/2} \approx 5.6 \times 10^{-12} \frac{\text{newtons}}{\text{m/sec}} \quad (\text{B29})$$

for $p = 6.5 \times 10^{-15}$ g/cm³ and $T = 300^\circ\text{K}$. The time constant m_B/p is about 1700 yr, so that

$$\langle \dot{x}_C^2 \rangle_{\text{av}} \approx (2pkT/m_B^2)t \quad (\text{B30})$$

$$\langle x_C^2 \rangle_{\text{av}} \approx (2pkT/3m_B^2)t^3 \approx (1.4 \times 10^{-31} \text{m}^2/\text{sec}^3)t^3 \quad (\text{B31})$$

After one year, the rms value of x_C would only be

$$\langle x_C^2 \rangle_{\text{av}}^{1/2} \approx 61 \mu \quad (\text{B32})$$

so that the effect of gas in the cavity is completely negligible.

Appendix C: Calculation or Estimation of Gyroscope Random Drifts

The equations of the gyrorotor in its principal axis system are given by

$$(1 - \epsilon_1)\dot{\omega}_{Bx} + \epsilon_2\omega_{By}\omega_{Bz} = M_{Bz}/C$$

$$(1 - \epsilon_2)\dot{\omega}_{By} - \epsilon_1\omega_{Bz}\omega_{Bx} = M_{By}/C \quad (\text{C1})$$

$$\dot{\omega}_{Bz} + (\epsilon_1 - \epsilon_2)\omega_{Bx}\omega_{By} = M_{Bz}/C$$

where the principal moments of inertia are $A = C(1 - \epsilon_1)$, $B = C(1 - \epsilon_2)$, and C . ϵ_1 and ϵ_2 are called the ellipticities and are of the order of 10^{-5} . If the terms involving ϵ_1 and ϵ_2

may be neglected, the equations of motion become, with $\mathbf{o}_B = \mathbf{e}_\omega \omega_B$,

$$\mathbf{M}_{1\parallel} = A \mathbf{e}_\omega \dot{\omega}_B \quad (\text{C2})$$

$$\mathbf{M}_{\perp} = \dot{\phi} \times A \omega_B = \dot{\phi} \times \mathbf{h}_B \quad (\text{C3})$$

where \mathbf{M}_{\parallel} , and \mathbf{M}_{\perp} are the components of the disturbing torque parallel to and perpendicular to ω_B , respectively. The magnitude of the drift rate is computed from Eq. (C3).

The principal model that will be used for most of the torque calculations is an almost spherical rotor of ellipsoidal shape. The eccentricities e_1 and e_2 are defined by

$$a^2 \triangleq c^2(1 + e_1)$$

$$b^2 \triangleq c^2(1 + e_2) \quad (\text{C4})$$

and the eccentricities and the ellipticities are related by

$$e_1 = 2\epsilon_1 \quad e_2 = 2\epsilon_2 \quad (\text{C5})$$

so that

$$a = c(1 + \epsilon_1) \quad b = c(1 + \epsilon_2) \quad (\text{C6})$$

It will be assumed for definiteness that

$$a > b > c \quad (\text{C7})$$

$$A < B < C \quad (\text{C8})$$

In some of the calculations (such as gravity gradient) and in the presentation of the results (as in Table 4), it is convenient to ignore the difference between ϵ_1 and ϵ_2 .

In each example below, the maximum value of the drift rate will be computed. In many cases, as for example with the gravity gradient torque, the actual drift will be less since part of the total effect of the torque will have zero time average.

Gravity Gradient Torque

If it is assumed that the spinning rotor may be represented by an oblate spheroid with moments of inertia $A = B = C(1 - \epsilon)$ and C , the peak drift rate is given by Cannon¹¹ as

$$\dot{\phi}_{\text{peak}} = \frac{3}{2}(\omega_0^2/\omega_B)\epsilon \quad (\text{C9})$$

ω_0 is the satellite orbit angular velocity and ω_B is the rotor spin angular velocity.

If the bulge is assumed to be due to a permanent bulge plus one caused by the rotation, then

$$\epsilon = \epsilon_P + \epsilon_R \quad (\text{C10})$$

It is shown in Klein and Sommerfeld³⁵ that

$$\epsilon_R = \frac{1}{8} \frac{5}{8} (\rho_m \omega_B^2 R_B^2 / E) \quad (\text{C11})$$

where E is Young's modulus for the material. Thus

$$\dot{\phi}_{\text{peak}} = \frac{45}{76} \frac{\omega_0^2 \rho_m R_B^2 \omega_B}{E} + \frac{3}{2} \frac{\omega_0^2}{\omega_B} \epsilon_P \quad (\text{C12})$$

If

$$\omega_B = \left(\frac{38}{15} \frac{E \epsilon_P}{R_B^2 \rho_m} \right)^{1/2} \approx 1.7 \times 10^3 \frac{\text{rad}}{\text{sec}} \quad (\text{C13})$$

for silicon, then $\dot{\phi}_{\text{peak}}$ has a minimum value of

$$\dot{\phi}_{\text{peak min}} = 3\omega_0^2 \left(\frac{15}{38} \frac{R_B^2 \rho_m \epsilon_P}{E} \right)^{1/2} \quad (\text{C14})$$

Electromagnetic Torques

The description of magnetic eddy currents in sphere is a classical problem and is discussed in Refs. 36–39. The eddy current torque tends to slow down the rotation of the gyro-

rotor, and it tends to precess the spin axis. For a silicon rotor in the earth's field, the time constant is given by

$$\text{time const} = \frac{4\rho_m}{B_{\perp}^2 \sigma} \approx 74,000 \text{ yr} \quad (\text{C15})$$

The peak precession rate is given by

$$\dot{\phi}_{\text{peak}} = B_{\parallel} B_{\perp} \sigma / 4\rho_m \approx 4.3 \times 10^{-13} \text{ rad/sec} \quad (\text{C16})$$

B_{\parallel} and B_{\perp} are the components of B parallel to and perpendicular to ω_B , respectively. This rate is 10 times too big to do the Pugh-Schiff experiment, but, since it falls off as the square of the field attenuation, a very simple magnetic shield would reduce it to an acceptable value.

The Barnett effect, Einstein-de Haas effect, and the Tolman effect are discussed by Harnwell,⁴⁰ and the spinning charge calculation is straightforward. The effect of elliptic geometry is covered in Stratton,⁴¹ and the magnetization integrals are easily evaluated by expanding in powers of e . The results in Stratton for a sphere in a uniform field are easily extended to the case of crystalline magnetic anisotropy and give a drift rate of

$$\dot{\phi}_{\text{peak}} = \frac{5B_0' H_0'' (\chi_m'' - \chi_m')}{2\rho_m R_B^2 \omega_S} \quad (\text{C17})$$

H_0 and B_0 are taken as constant external fields, and the single and double primes represent their components along mutually perpendicular body principal axes. χ_m' and χ_m'' are the eigenvalues of the χ_m tensor for the prime and double prime axes, respectively.

The drift rate produced by induced electric moments and by charge on an ellipsoid may be bounded by the following procedure. The torque on an uncharged ellipsoid in a non-uniform external electric field is given by

$$\mathbf{M} = \frac{\epsilon_0}{2} \int_{\text{surface}} E^2 \mathbf{r} \times d\mathbf{S}_B \quad (\text{C18})$$

since the electric field is normal to the surface. For example, the y component of \mathbf{M} is

$$M_y = \frac{\epsilon_0}{2} \int_{\text{surface}} E^2 \frac{x_B z_B [(1/a^2) - (1/c^2)] dS_B}{[(x_B^2/a^4) + (y_B^2/b^4) + (z_B^2/c^4)]^{1/2}} \quad (\text{C19})$$

$$= -e_1 \frac{\epsilon_0}{2c^2(1 + e_1)} \times$$

$$\int_{\text{surface}} \frac{E^2 x_B z_B dS_B}{[(x_B^2/a^4) + (y_B^2/b^4) + (z_B^2/c^4)]^{1/2}} \quad (\text{C20})$$

Since the ellipsoid is almost spherical, the radical may be replaced by $1/c$. Then only errors of the order of e_1 and e_2 are introduced. Hence

$$M_y \approx \frac{-e_1 \epsilon_0}{2c} \int_{\text{surface}} E^2 x_B z_B dS_B \quad (\text{C21})$$

Since the maximum value of $x_B z_B$ differs from $c^2/2$ only by terms of order e_1 and e_2 ,

$$|M_y| < \pi \epsilon_0 E_{av}^2 c^2 e_1 \quad (\text{C22})$$

$\dot{\phi}_{\text{peak}}$ due to M , is given by

$$\dot{\phi}_{\text{peak}} < \frac{15}{4} \frac{\epsilon_0 E_{av}^2 e_1}{\rho_m R_B^2 \omega_S} \quad (\text{C23})$$

with similar relations for the other axes. By a similar technique, it is possible to obtain bounds on the drift rates due to charge on an ellipsoid, sensor radiation pressure, and gas in the cavity.

The surface electric eddy currents are due to the fact that the charge distribution of a charged ellipsoid in an electric field must vary as the orientation of the ellipsoid varies. The results quoted in Table 4 are estimates based on the approximation that a fraction, e_1 or e_2 , or the total charge circulates around the ellipsoid at a frequency $\omega_B/2\pi$.

Gas Torques

The gas in the cavity tends to slow down the rotation and to precess the spin axis. The resistance is approximately proportional to ω_S and may be computed from kinetic theory. For the purpose of an order of magnitude estimate, b will be taken as

$$b = (\pi/9) R_B^4 \rho (3kT/m_{av})^{1/2} \approx 1.8 \times 10^{-16} \text{ joule-sec} \quad (\text{C24})$$

The spin-down time constant due to b can be computed from the equation

$$C\dot{\omega}_B + b\omega_B = M_{\parallel} \quad (\text{C25})$$

and the result is

$$\text{spin-down time const} = C/b \approx 2200 \text{ yr} \quad (\text{C26})$$

The random walk of the spin axis may be evaluated by the same procedure as that outlined in Appendix B. The rms drift angle of the spin axis is given by

$$\langle \phi^2 \rangle_{av} = (2bkT/h_B^2)t \quad (\text{C27})$$

Equation (C27) predicts a drift of

$$\langle \phi^2 \rangle_{av}^{1/2} \approx 5.4 \times 10^{-13} \text{ rad} \quad (\text{C28})$$

in one year which is entirely negligible.

References

- ¹ Gerathewohl, S. J., "Zero-G devices and weightlessness simulators," National Academy of Sciences—National Research Council, Publication 781 (1961).
- ² Ericke, K. A., "The satelloid," *Astronaut. Acta* 2, Fasc. 2, 63–100 (1956).
- ³ Dicke, R. H., "The nature of gravitation," *Science in Space*, edited by L. V. Beoknev and H. Odishaw (McGraw-Hill Book Co., Inc., New York, 1961), Part 2, pp. 91–118.
- ⁴ Pugh, G. E., "Proposal for a satellite test of the Coriolis prediction of general relativity," Weapons Systems Evaluation Group Res. Memo. 11, The Pentagon, Washington, D. C. (November 12, 1959).
- ⁵ MacDonald, G. J. F. and Cohan, B. F., "Sustaining orbiting geophysical observatory," unpublished proposal, Institute of Geophysics and Planetary Physics, Univ. of California at Los Angeles (December 1962).
- ⁶ Proceedings of the Conference on Experimental Tests of the Theories of Relativity, unpublished, Stanford Univ. (July 1961), pp. 61–65.
- ⁷ Kaula, W. M., "Celestial geodesy," NASA TN D-1155 (March 1962).
- ⁸ Jacchia, L. G., "Variations in the earth's upper atmosphere as revealed by satellite drag," *Rev. Mod. Phys.* 35, 973–991 (1963).
- ⁹ Sharp, G. W., Hanson, W. B., and McKibbin, D. D., "Atmospheric density measurements with a satellite borne microfilm gauge," *J. Geophys. Res.* 67, 375–382 (1962).
- ¹⁰ Schiff, L. I., "Motion of a gyroscope according to Einstein's theory of gravitation," *Proc. Natl. Acad. Sci. U. S.* 20, 1288–1302, 1405–1421, 1517–1532 (1959).
- ¹¹ Cannon, R. H., Jr., "Requirement, and design for a special gyro for measuring general relativity effects from an astronomical satellite," *Kreiselprobleme*, edited by H. Ziegler (Springer-Verlag, Berlin, 1963), pp. 146–160.
- ¹² Dicke, R. H., Hoffmann, W. F., and Krotkov, R., "Tracking and orbit requirements for experiment to detect variations in gravitational constant," *Space Research II—Proceedings of the Second International Space Science Symposium* (Interscience Publishers, Inc., New York, 1961), pp. 287–291.
- ¹³ Rider, L., "Impulsive orbit sustaining techniques for low altitude satellites," Aerospace Corp. TR T.N. 594-1105-2 (December 5, 1960).
- ¹⁴ Bruce, R. W., "Satellite orbit sustaining techniques," *ARS J.* 31, 1237–1241 (1961).
- ¹⁵ Roberson, R. E., "An intermittent orbit sustaining technique," *Astronaut. Acta* 8, Fasc. 1, 42–48 (1962).
- ¹⁶ Smelt, R., "Upper atmosphere properties derived from Discoverer satellites," TR SUDAER 111, Dept. of Aeronautics and Astronautics, Stanford Univ. (1961).

- ¹⁷ Sissenwine, N., "Announcing the U. S. standard atmosphere—1962," *Astronautics* **7**, 52–53 (August 1962).
- ¹⁸ Flugge-Lotz, I., *Discontinuous Automatic Control* (Princeton University Press, Princeton, N. J., 1953), Chap. 4.
- ¹⁹ Graham, D. and McRuer, D., *Analysis of Nonlinear Control Systems* (John Wiley and Sons, Inc., New York, 1961), pp. 370–393.
- ²⁰ Flugge-Lotz, I., "Discontinuous automatic control," *Appl. Mech. Rev.* **14**, 581–584 (1961).
- ²¹ Gaylord, R. S. and Keller, W. N., "Attitude control system using logically controlled pulses," *ARS Progress in Astronautics and Rocketry: Guidance and Control*, edited by R. E. Roberson and J. S. Fariior (Academic Press, New York, 1962), Vol. 8, pp. 629–648.
- ²² Dahl, P. R., Aldrich, G. T., and Herman, L. K., "Limit cycles in reaction jet attitude control systems subject to external torques," *ARS Progress in Astronautics and Rocketry: Control and Guidance*, edited by R. E. Roberson and J. S. Fariior (Academic Press, New York, 1962), Vol. 8, pp. 599–628.
- ²³ Smart, W. M., *Celestial Mechanics* (Longmans Green and Co., Inc., London, 1953), pp. 291 f.
- ²⁴ Wheelon, A. D., "An introduction to mid-course and terminal guidance," Space Technology Labs. Rept. G.M.-T.M.-0165-00252 (June 10, 1958).
- ²⁵ Geyling, F. T., "Satellite perturbations from extra-terrestrial gravitation and radiation pressure," *J. Franklin Inst.*, 375407 (May 1960).
- ²⁶ Eggleston, J. M. and Beck, H. D., "A study of the positions and velocities of a space station and a ferry vehicle during rendezvous and return," NASA TR R-87 (1961).
- ²⁷ Tempelman, W. H., "Circular orbit partial derivatives," *AIAA J.* **1**, 1187–1189 (1963).
- ²⁸ Aseltine, J. A., *Transform Method in Linear System Analysis* (McGraw-Hill Book Co., Inc., New York, 1958), pp. 73–75.

- ²⁹ Kane, T. R., Marsh, E. L., and Wilson, W. G., Letter to the *J. Astronaut. Sci.* **9**, 108–109 (Winter 1962).
- ³⁰ Jeans, J., *The Mathematical Theory of Electricity and Magnetism* (The University Press, Cambridge, England, 1960), pp. 167–168.
- ³¹ Bandeen, W. R. and Manger, W. P., "Angular motion of the spin axis of Tiros I meteorological satellite due to magnetic and gravitational torques," *J. Geophys. Rev.* **65**, 2992–2995 (1960).
- ³² Engstrom, R. W., "Multiplier photo-tube characteristics: application to low light levels," *J. Opt. Soc. Am.* **37**, 420 (1947).
- ³³ Aseltine, J. A., Ref. 28, pp. 240–241.
- ³⁴ Kennard, E. H., *Kinetic Theory of Gases* (McGraw-Hill Book Co., Inc., New York, 1938), pp. 280–283.
- ³⁵ Klein, F. and Sommerfeld, A., *Theorie des Kreisels, Heft III, Die Störenden Einflüsse. Astronomische und Geophysikalische Anwendungen* (Leipzig, Druck und Verlag, von G. B. Teubner, 1903), pp. 692–696.
- ³⁶ Smythe, W. R., *Static and Dynamic Electricity* (McGraw-Hill Book Co., Inc., New York, 1950), p. 398.
- ³⁷ Houston, W. V. and Muench, N., "Electromagnetic forces on a superconductor," *Phys. Rev.* **79**, 967–970 (1950).
- ³⁸ Alers, P. B., McWhirter, J. W., and Squire, C. F., "Eddy currents and supercurrents in rotating metal spheres at liquid helium temperatures," *Phys. Rev.* **84**, 104–107 (1951).
- ³⁹ Tabakin, F., "Torque on a spinning metallic sphere induced by a time dependent magnetic field," TR BSD-61-25, Space Technology Labs., Inc., Los Angeles, Calif. (September 1961).
- ⁴⁰ Harnwell, G. P., *Principles of Electricity and Electromagnetism* (McGraw-Hill Book Co., Inc., New York, 1949), pp. 377–381.
- ⁴¹ Stratton, J. A., *Electromagnetic Theory* (McGraw-Hill Book Co., Inc., New York, 1941), pp. 201–217.